



Testing the Seamount Refuge Hypothesis for Predators and Scavengers in the Western Clarion-Clipperton Zone

Astrid B. Leitner^{1,2*}, Jeffrey C. Drazen² and Craig R. Smith²

¹ Monterey Bay Aquarium Research Institute, Moss Landing, CA, United States, ² Department of Oceanography, University of Hawai'i at Mānoa, Honolulu, HI, United States

OPEN ACCESS

Edited by:

Daphne Cuvelier,
Center for Marine and Environmental
Sciences (MARE), Portugal

Reviewed by:

Frine Cardone,
Anton Dohrn Zoological Station, Italy
Rui Pedro Vieira,
Centre for Environment, Fisheries
and Aquaculture Science (CEFAS),
United Kingdom

*Correspondence:

Astrid B. Leitner
aleitner@mbari.org

Specialty section:

This article was submitted to
Deep-Sea Environments and Ecology,
a section of the journal
Frontiers in Marine Science

Received: 01 December 2020

Accepted: 26 July 2021

Published: 19 August 2021

Citation:

Leitner AB, Drazen JC and
Smith CR (2021) Testing the
Seamount Refuge Hypothesis
for Predators and Scavengers
in the Western Clarion-Clipperton
Zone. *Front. Mar. Sci.* 8:636305.
doi: 10.3389/fmars.2021.636305

Seamounts are common in all ocean basins, and most have summit depths >3,000 m. Nonetheless, these abyssal seamounts are the least sampled and understood seamount habitats. We report bait-attending community results from the first baited camera deployments on abyssal seamounts. Observations were made in the Clarion Clipperton Zone (CCZ), a manganese nodule region stretching from south of Hawaii nearly to Mexico. This zone is one of the main target areas for (potential) large-scale deep-sea nodule mining in the very near future. The Seamount Refuge Hypothesis (SRH) posits that the seamounts found throughout the CCZ provide refugia for abyssal fauna likely to be disturbed by seabed mining, yielding potential source populations for recolonization of mined areas. Here we use baited cameras to test a prediction of this hypothesis, specifically that predator and scavenger communities are shared between abyssal seamounts and nearby abyssal plains. We deployed two camera systems on three abyssal seamounts and their surrounding abyssal plains in three different Areas of Particular Environmental Interests (APEIs), designated by the International Seabed Authority as no-mining areas. We found that seamounts have a distinct community, and differences in community compositions were driven largely by habitat type and productivity changes. In fact, community structures of abyssal-plain deployments hundreds of kilometers apart were more similar to each other than to deployments ~15 km away on seamounts. Seamount communities were found to have higher morphospecies richness and lower evenness than abyssal plains due to high dominance by synphobranchid eels or penaeid shrimps. Relative abundances were generally higher on seamounts than on the plains, but this effect varied significantly among the taxa. Seven morphotypes were exclusive to the seamounts, including the most abundant morphospecies, the cutthroat eel *Ilyophis arx*. No morphotype was exclusive to the abyssal plains; thus, we cannot reject the SRH for much of the mobile megafaunal predator/scavenging fauna from CCZ abyssal plains. However, the very small area of abyssal seamounts compared to abyssal plains suggest that seamounts are likely to provide limited source populations for recolonizing abyssal plains post-mining

disturbance. Because seamounts have unique community compositions, including a substantial number of predator and scavenger morphospecies not found on abyssal plains, they contribute to the beta biodiversity of the Clarion-Clipperton Zone, and thus indirect mining impacts on those distinct communities are of concern.

Keywords: seamount, baited camera, deep-sea, scavenger, CCZ, nodule

INTRODUCTION

Seamounts are submarine mountains that rise at least 1,000 m above the surrounding seafloor (Pitcher et al., 2007). Seamounts are common seafloor features, with tens to hundreds of thousands of seamounts estimated globally (Kim and Wessel, 2011; Yesson et al., 2011). Seamounts are still understudied habitats, but current data suggest that seamounts with summits shallower than 3000 m are often characterized by rich benthic and demersal megafaunal communities with high abundance, high biomass, and high diversity (Pitcher et al., 2007; Morato et al., 2010; Schlacher et al., 2010). The vast majority of these features are small, deep seamounts, but these are also the least studied and least understood class of seamounts (Wessel, 2001; Kim and Wessel, 2011).

The Clarion-Clipperton Zone (CCZ), a large region rich in polymetallic nodules in the eastern equatorial Pacific between Hawaii and Mexico, is currently being considered for deep seabed nodule mining. The International Seabed Authority (ISA) is responsible for environmental management in the CCZ and to that end has established nine, 400 km × 400 km no-mining zones called Areas of Particular Environmental Interest (APEIs; Wedding et al., 2013). The APEIs were designed as a representative system of protected areas to cover the biophysical gradients in productivity, nodule cover, and depth across the CCZ, as well as to protect the range of seafloor habitat types in the CCZ, including abyssal hills and seamounts (Wedding et al., 2013). The CCZ hosts approximately 221 seamounts, whose average summit depth is 2850 m below sea-level (data extracted from Yesson et al., 2011; **Figure 1**). It has recently been hypothesized that these seamounts, which will be spared from direct mining activities due to the rugosity and complexity of their terrain, may provide refugia for many species from the abyssal plain displaced or disturbed by mining and thus may provide source populations for recolonization of mined areas (Cuvelier et al., 2020). A prediction of this hypothesis is that seamounts and nearby abyssal plains share a substantial proportion of their fauna. Thus far, this hypothesis, referred to throughout this manuscript as the Seamount Refuge Hypothesis (SRH), has been evaluated and rejected for benthic megafauna (excluding highly mobile groups like fishes and crustaceans) in the eastern CCZ, where only 10% of fauna were observed on both seamounts and plains (Cuvelier et al., 2020). In addition, a recent study using a multi-gene environmental DNA metabarcoding approach, suggests substantial differences in metazoan communities with limited taxonomic overlap between seamounts and plains in the western CCZ (Laroche et al., 2020). However, an evaluation specific to fishes and other mobile top predators and scavengers is still lacking.

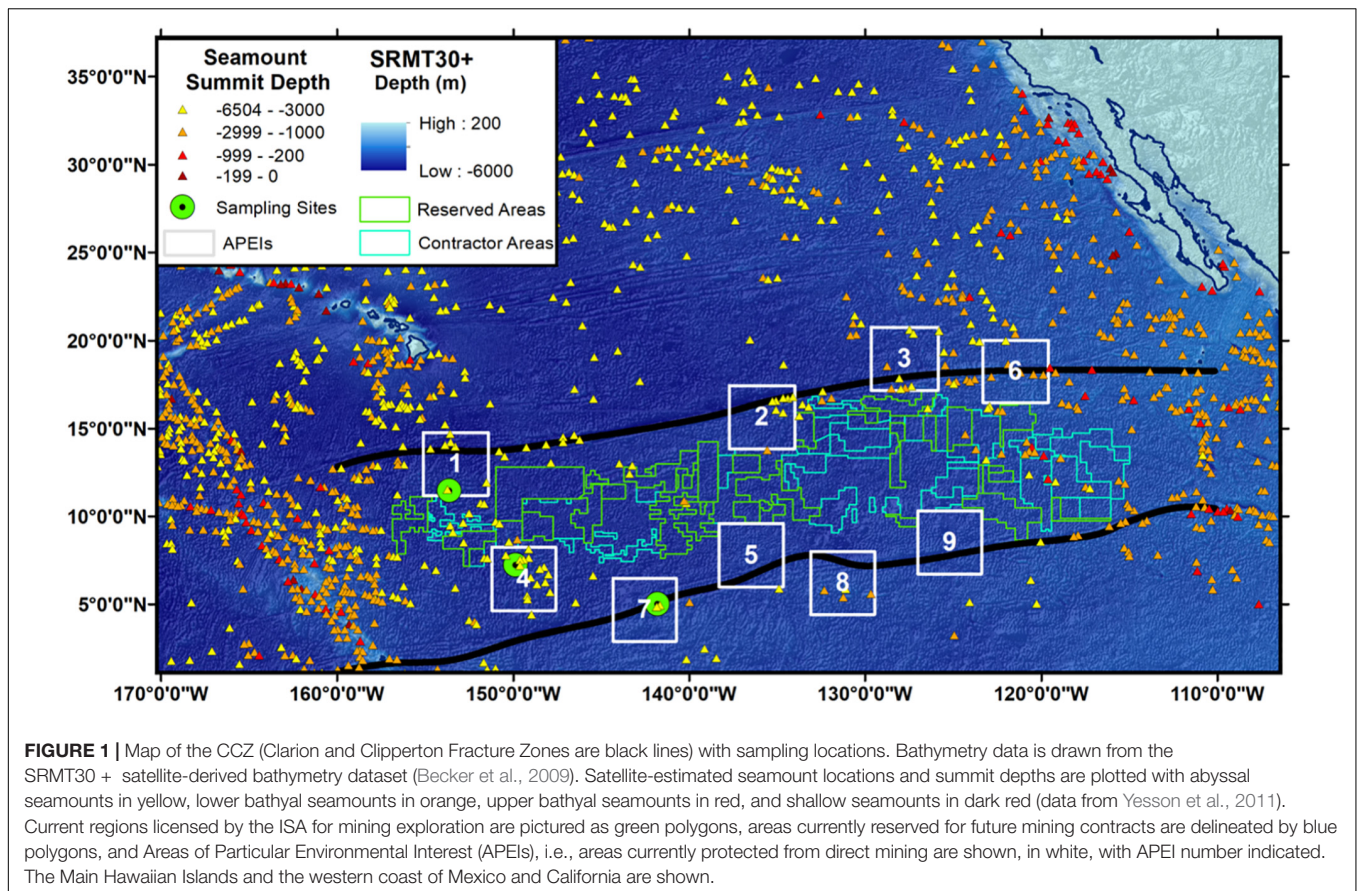
Knowledge of the distribution, ecology, and behavior of top predators is crucial to establish environmental baselines and conduct ecosystem-based management (Estes et al., 2011; Wedding et al., 2015, 2013). Even at low densities, predators can exert top-down control on prey populations, thereby controlling prey abundance, biomass, and diversity, and influencing habitat use/choice and behavior of prey (Myers et al., 2007; Polovina et al., 2009; Estes et al., 2011; Drazen and Sutton, 2017). In the CCZ, top seafloor predators are large fishes, crustaceans, and octopods, many of which are opportunistic scavengers readily attracted to baited cameras (Leitner et al., 2017; Drazen et al., 2019; Harbour et al., 2020). While these highly mobile predators are also detected in seafloor imaging transects, they are often observed in a very low (<1%) percentage of images (e.g., Milligan et al., 2016) due to their sparse distribution and avoidance of light, noise, and vibrations from survey vehicles, making baited imaging a key technique for studying the predator-scavenger component of abyssal seafloor ecosystems (Drazen et al., 2021, this vol.; Leitner et al., 2017).

Here we test the “shared-fauna” prediction of the SRH for bait-attending fauna in the western CCZ using data from two baited camera landers which were deployed a total of 17 times on three different seamounts and their proximate abyssal plains, one in each of the three western APEIs. Collectively, the DeepCCZ expedition has provided the first baited camera data from the western APEI regions. The data presented here also represent the first baited experiments on abyssal-depth seamounts. Thus, in addition to evaluating the SRH, we also report on the diversity and composition of the bait-attending megafauna and the potential importance of environmental characteristics such as seafloor habitat type and productivity in structuring this community.

MATERIALS AND METHODS

Study Site

Data were collected during the DeepCCZ cruise to the western CCZ aboard the R/V Kilo Moana in May-June of 2018 (**Figure 1**). All sampling took place within three APEIs: APEI 1, APEI 4, and APEI 7 (north to south, **Figures 2A–C**). These APEIs lie on a strong primary productivity gradient. APEI 7, the southernmost, is under the influence of equatorial upwelling with a decadal average chlorophyll-a concentrations of 0.15 mg m⁻³ Chl-a [National Oceanic & Atmospheric Administration (NOAA), and National Aeronautics and Space Administration (NASA), n.d.] and an estimated average particulate organic carbon (POC) flux to depth of 1.9 mg C_{org} m⁻² d⁻¹ (Lutz et al., 2007). The mid-latitude APEI, APEI 4, is characterized by lower surface



chlorophyll concentrations and seafloor POC flux (0.12 mg m^{-3} Chl-a and $1.4 \text{ mg } C_{org} \text{ m}^{-2} \text{ d}^{-1}$). The northernmost APEI, APEI 1, is in the least productive waters with just 0.07 mg m^{-3} Chl-a and an estimated average seafloor POC flux of $1.1 \text{ mg } C_{org} \text{ m}^{-2} \text{ d}^{-1}$.

One abyssal seamount was selected in each APEI to test the SRH. Because these APEIs were all unmapped and unsampled prior to the expedition, seamount targets were selected from the best available satellite-estimated bathymetry: the Shuttle Radar Topography Mission (SRTM30+) 30 arc-second global bathymetry grid (Becker et al., 2009), which combines both high resolution ($\sim 1 \text{ km}$) ship-based bathymetry data and $\sim 9 \text{ km}$ satellite-gravity data.¹ Seamounts were chosen to have elevations between 1,000 and 1,500 m above the surrounding seafloor and summits at abyssal depths ($> 3,000 \text{ m}$) to meet the classic definition of “seamount” (Pitcher et al., 2007) while still minimizing differences in community composition stemming from depth distributions. During the cruise, each seamount was mapped at 50 m resolution using shipboard multibeam sonar (see details below).

After mapping of the initial seamount target in APEI 7, additional seamount targets were selected to be as similar to the first as possible, with roughly similar summit depths, elevations, and geomorphologies. All were elongated, ridge-like

features. Lander deployment locations on the seamount summits were strategically chosen to be in large, flat areas to allow for successful lander deployments. Landers were deployed in soft sediment habitats on both seamounts and proximate abyssal plains. Seamount effects on benthic larval distributions have been documented to extend 7 km away from shallow seamount summits, and possibly as far as 40 km (Mullineaux and Mills, 1997), and island effects on productivity extend up to 30 km from shore declining exponentially with distance (Gove et al., 2016). While seamount effect radius is not known for abyssal seamounts, the radius is likely much smaller given the low average current speeds at abyssal depths; thus a 15 km seamount buffer (more than twice the documented shallow seamount effect and half the island mass effect) was instituted such that all abyssal plain deployments were $> 15 \text{ km}$ from the seamount summit ridgeline and well out onto the abyssal plain (Figure 2).

Data Collection

Bathymetric data was collected at 50 m resolution using the R/V Kilo Moana’s deep-water multibeam system (12 kHz Simrad EM120) at a constant ship speed of eight knots. Raw pings were manually edited in near real time with the software Qimera^R. Sound velocity profiles (SVP) were taken every 6 h during surveys. Processed multibeam bathymetry was then used to find suitable lander deployment sites (large, flat areas atop each seamount) and for subsequent spatial analysis in ArcGIS 10.4.

¹https://topex.ucsd.edu/WWW_html/srtm30_plus.html

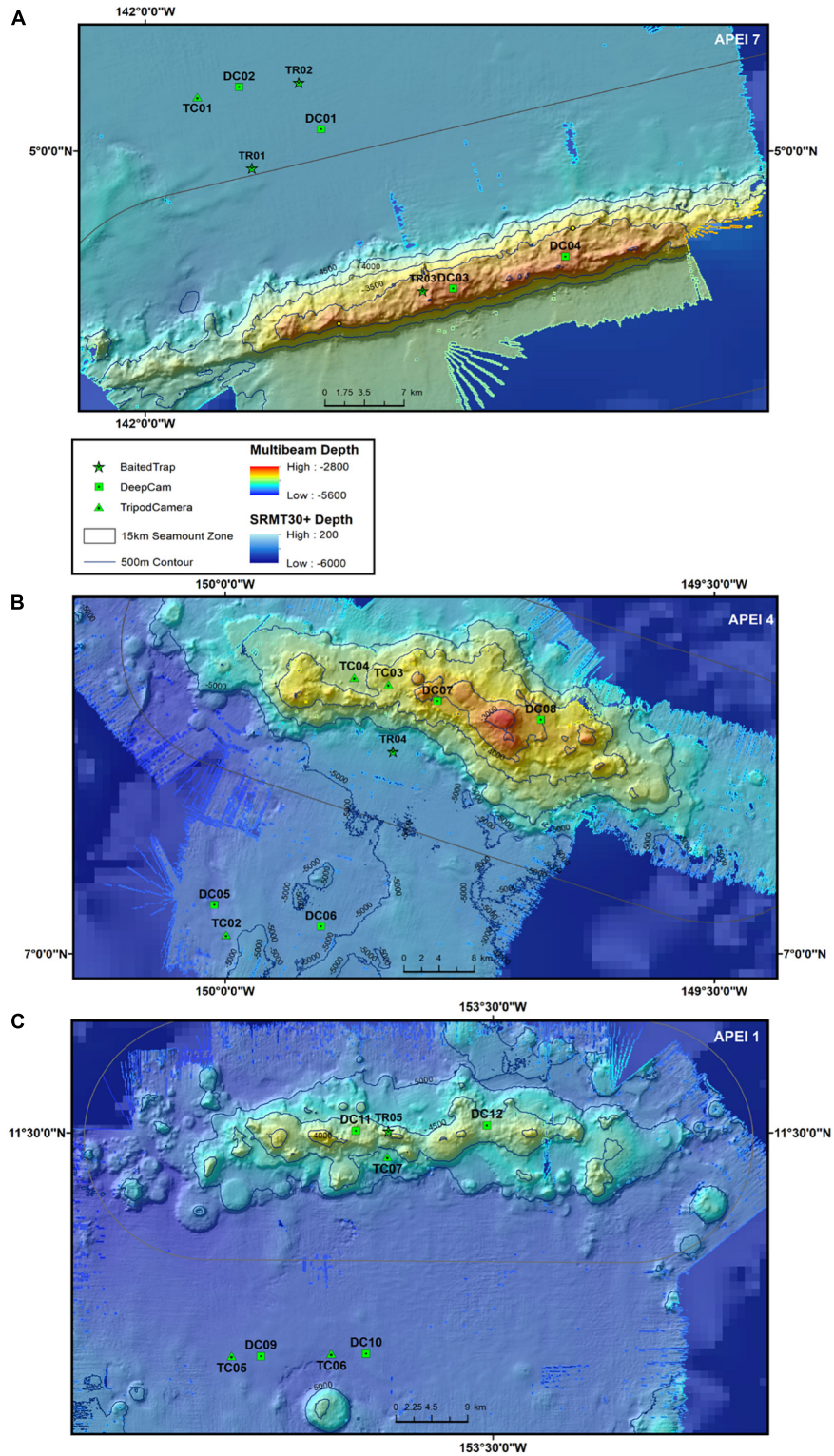


FIGURE 2 | Detailed multibeam bathymetry and sampling locations from three APEIs **(A)** APEI 7, **(B)** APEI 4, **(C)** APEI 1. Baited trap (TR) deployment locations (stars) and baited camera deployment locations [DeepCam lander deployments (DC) as squares, Tripod Camera Lander (TC) as triangles] are shown in each panel. Finer scale multibeam bathymetry (rainbow color scale) overlays coarser satellite-estimated bathymetry (blue, pixelated color scale). The “seamount zone” denoted by a 15 km buffer (as measured from the seamount ridge-line) is shown in gray. Depth contours (500 m) are shown in black. Note TC01 (the first tripod deployment) was not successful.

Two baited-camera landers were used to collect seafloor imagery. The first, DeepCam (DC), is a baited, geometrically calibrated stereo-video system. Details of this system are described elsewhere (Leitner et al., 2017) but in brief, two identical cameras were mounted with an overlapping horizontal field of view at a slightly downward angle at 0.56 m above the seafloor. Geometric calibration (done using the CAL software by SeaGIS)² provided a precise estimation of the seafloor area within the field of view that was illuminated by the system's lights (1.86 m²). To minimize light disturbance on bait-attending fauna and maximize battery life, videos were recorded for 2-min intervals (clips) interrupted by 8-min lights-off intervals. This lander was also equipped with a Nortek Aquadopp 6000 current meter, though this instrument was lost during the ninth recovery. The current meter provided true bottom depth, bottom temperature, and current velocities. Videos from both synchronous cameras were annotated using the EventMeasure software by SeaGIS for all visible megafauna to the lowest taxonomic level possible, although only bait-attending (scavengers and necrophagivores) fauna are considered in the analysis. Identifications were made using the collaborative CCZ abyssal photographic fish guide, published as supplementary material to Drazen et al. (2021, this vol.). This guide provides an image-based identifications and ensures naming standardization across the greater CCZ region (Drazen et al., 2021, this vol.). As such, all taxa are considered morphospecies except in a few instances, where concurrent capture of specimens allowed for confirmation of image-based identification (e.g., *Ilyophis arx*). MaxN, a conservative relative abundance metric, was extracted for each clip and for each deployment for each bait-attending taxon (Cappo et al., 2006). MaxN represents the maximum number of individuals of each single taxon present in a single frame of a clip (clipwise MaxN) or deployment (dropwise MaxN). MaxN eliminates the possibility of double counting individuals over the course of a video, and is therefore a conservative relative abundance metric.

The second lander, Tripod Camera (TC), is a deep-sea time-lapse photography camera tripod described in Ziegler et al. (2020). Camera angle and elevation were modified to match the DC to make the two systems as comparable as possible. This lander took one still photograph every minute. Because of the horizontal camera angle and lack of stereo calibration, a precise estimate of the seafloor area in view is not possible. By comparing images between landers, the field of view of the Tripod lander was determined to be slightly smaller than that of the DC. Still images were annotated manually to the lowest taxonomic level possible for all visible megafauna, though only bait-attending fauna were used in analyses. It should be noted that species level identification is more challenging for still photos than for video, especially for the large, red decapod shrimps (known from the DC to be a mix of penaeid and aristeid shrimps), necessitating a taxa that combines the two as a single morphospecies for comparison across landers. MaxN was extracted for each deployment (dropwise MaxN) for subsequent analyses.

²www.seagis.com.au

Both landers were baited with ~1 kg of Pacific mackerel (*Scomber japonicus*), positioned 1.5 m in front of the cameras. This resulted in a complete view of the entire area around the bait package in the DC video. For the Tripod, the field of view included only the bait package and the seafloor beyond it. Deployment times for landers ranged from 12.7 to 44.2 h (Table 1).

Finally, whenever possible given shiptime constraints, a baited trap (details provided in Leitner et al., 2017) was deployed to collect voucher specimens for morphological and genetic identification. To minimize interactions between the bait plumes of the three landers, simultaneous deployments were spaced at least 4 km apart.

Statistics

The “shared-fauna” prediction of the SRH was evaluated for bait-attending fauna (scavengers and predators) by comparing taxonomic overlap, diversity metrics, and community composition between seamounts and proximate abyssal plains at the three APEIs in the western CCZ.

Diversity and Taxonomic Overlap

In order to evaluate differences in diversity, rarified and extrapolated abundance-based Hill numbers ($q = 0, 1, 2$) were compared between habitat (seamount vs. abyssal plain) and APEI using the {iNEXT} R package (Chao et al., 2014; Hsieh et al., 2016). Hill numbers correspond to morphospecies richness ($q = 0$), Shannon diversity ($q = 1$), and Simpson diversity ($q = 2$). Significant differences in diversity metrics were evaluated using the bootstrapped 95% confidence intervals (CI) around the sampling curves, such that non-overlapping CI around each curve were interpreted as significant differences (Chao et al., 2014; Hsieh et al., 2016). To evaluate data coverage, morphospecies accumulation curves were also compared between seamounts and abyssal plains and between APEIs. To evaluate morphospecies overlaps across APEI and habitat type, morphospecies intersections were visualized and quantified for each station (APEI and habitat combination) using the {UpSetR} package (Gehlenborg, 2019). Taxonomic overlap uses taxon-presence data to compare how many taxa are shared between different sites. It is reported in percent overlap, in this case the percentage of the total number of observed morphospecies that are shared between sites.

Community Analysis

In order to visualize and quantify differences in community composition across all deployments and specifically across habitat types, a constrained ordination based on a Bray-Curtis dissimilarity matrix calculated from the square root transformed relative abundances (MaxN) of all bait-attending taxa ($N = 20$) was run using the capscale function in the R package {vegan} (Oksanen et al., 2015). Capscale performs a principal coordinates analysis (PCoA) and then uses given predictors to conduct an eigenanalysis to determine the axes along which the predictor explains as much of the dissimilarity between communities as possible (Oksanen et al., 2015). Permutations ($N = 9,999$) were stratified by APEI to account for the spatial

TABLE 1 | Metadata and deployment information for all lander deployments.

| Drop | Stratum | Habitat Type | Lander | Image Type | Imaging Interval | Duration | Latitude | Longitude | Depth |
|-------|--------------|----------------|-------------|------------|------------------|----------|----------|-----------|--------|
| | | | | | (min) | (hr) | (dd N) | (dd E) | (m) |
| DC1 | APEI7 | Abyssal Plain | DeepCam | video | 2(10) | 23.9 | 5.018 | -141.860 | 4878.3 |
| DC2 | | Abyssal Plain | DeepCam | video | 2(10) | 28.3 | 5.053 | -141.926 | 4859.9 |
| DC3 | | Seamount | DeepCam | video | 2(10) | 16.4 | 4.884 | -141.755 | 3083.4 |
| DC4 | | Seamount | DeepCam | video | 2(10) | 17.6 | 4.911 | -141.666 | 3140.4 |
| DC5 | APEI4 | Abyssal Plain | DeepCam | video | 2(10) | 20.5 | 7.052 | -150.011 | 5216.5 |
| DC6 | | Abyssal Plain | DeepCam | video | 2(10) | 21.2 | 7.029 | -149.902 | 5003.7 |
| DC7** | | Seamount | DeepCam | video | 2(10) | 21.7** | 7.270 | -149.783 | 3541.8 |
| DC8 | | Seamount | DeepCam | video | 2(10) | 44.2 | 7.250 | -149.677 | 3496.8 |
| TC02 | | Abyssal Plain | Tripod | stills | 1 | 21.3 | 7.020 | -149.999 | 5096 |
| TC03 | | Seamount | Tripod | stills | 1 | 17.6 | 7.287 | -149.833 | 3885 |
| TC04 | | Seamount | Tripod | stills | 1 | 29.9 | 7.295 | -149.868 | 4134 |
| DC9 | APEI1 | Abyssal Plain | DeepCam | video | 2(10) | 43.1 | 11.249 | -153.761 | 5236 |
| DC10 | | Abyssal Plain | DeepCam | video | 2(10) | 23.4 | 11.252 | -153.643 | 5213 |
| DC11 | | Seamount | DeepCam | video | 2(10) | 18.4 | 11.502 | -153.654 | 4218 |
| DC12 | | Seamount | DeepCam | video | 2(10) | 12.7 | 11.508 | -153.507 | 4346 |
| TC05 | | Abyssal Plain | Tripod | stills | 1 | 18.3 | 11.250 | -153.794 | 5225 |
| TC06 | | Abyssal Plain | Tripod | stills | 1 | 18.4 | 11.252 | -153.682 | 5249 |
| TC07 | | Seamount | Tripod | stills | 1 | 17.6 | 11.473 | -153.619 | 4622 |
| TR01 | APEI7 | Abyssal Plain | Baited Trap | - | - | 30.7 | 4.985 | -141.915 | 4872 |
| TR02 | | Abyssal Plain | Baited Trap | - | - | 47.1 | 5.057 | -141.878 | 4871 |
| TR03 | | Seamount | Baited Trap | - | - | 25.1 | 4.883 | -141.779 | 3203 |
| TR04 | APEI4 | Abyssal Plain* | Baited Trap | - | - | 43.3 | 7.216 | -149.828 | 4872 |
| TR05 | APEI1 | Seamount | Baited Trap | - | - | 22.7 | 11.502 | -153.617 | 4175 |

Imaging interval for the DeepCam lander is 2 min of video during every 10 min.

*Within 15 km seamount buffer zone.

**Bait was consumed on initial descent, and so this deployment was almost entirely unbaited and therefore excluded from quantitative analyses.

dependence in the data. Significant clusters of deployments ($p < 0.05$) were identified using similarity profile analysis (SIMPROF) using the `simprof` function in the `{clustsig}` R package (Whitaker and Christman, 2014).

The predictors used to constrain the ordination were broad-scale benthic position index (BBPI), Lutz et al. (2007) estimates of seafloor POC flux at the drop locations, nodule abundance in the camera view, latitude, and lander type. Benthic position index (BPI), whether broad BBPI or fine scale (FBPI), is a relative position index defined as the difference in elevation between the location of interest (given as radius of cells around the sampling location) and the surrounding area (outer radius) (Modeler, 2012). Positive BPI values correspond to local high points, negative values correspond to local depressions, and values close to zero either represent flat areas or areas of constant slope (Lundblad et al., 2006; Verfaillie et al., 2007). BPI provides a continuous variable for quantifying bathymetric habitat differences. BBPI was calculated using GEBCO bathymetry data interpolated to 1 km² with the (McQuaid et al., 2020) PDC Mercator projection. The inner radius was 1 bathymetry cell and the outer radius was 100 cells (scale factor = 100 km). Using a coarse resolution bathymetry allowed for a single BBPI layer to be calculated across the dataset. This method successfully captured the habitat differences between abyssal plain deployments (BBPI \leq 25) and seamounts (BBPI \geq 500) in all three APEIs (Table 2). FBPI was calculated

from fine-scale (50 m) multibeam bathymetry for each APEI and was standardized for comparison across all three strata. However, because of seamount deployment locations in large, flat areas surrounded by higher elevations, FBPI was similar between seamount and abyssal plain deployments and was not used as a predictor. Estimated POC flux was derived from the Lutz et al. (2007) model. POC flux was highly correlated with longitude (Pearson correlation = 0.99) and with all surface productivity metrics (monthly average Chl-a concentration: 0.84, yearly average Chl-a concentration: 0.95, decadal average Chl-a concentration: 0.94). Because POC flux to depth is a good proxy for deep seafloor food availability (Smith et al., 2008), it was included while other correlated predictors (including longitude) were excluded. Nodule abundance was roughly estimated for each deployment using pixel image color analysis for each deployment. For the most consistent and evenly illuminated portion of the field of view, the proportion of that area that was covered by nodules was calculated with an online color-extraction tool set to 5 colors and a delta of 24.³ Latitude was also included as a predictor in the analysis because seafloor depth gets deeper with increasing latitude, and depth is too highly correlated to BBPI for both predictors to be included in the same model. Therefore, while habitat related differences in depth are captured by BBPI and habitat type, latitude is used to account for this depth

³http://www.coolphptools.com/color_extract#demo

TABLE 2 | Environmental characteristics for all camera deployments.

| Drop | Station Name | Depth | BBPI | FBPI | POC | Decadal Avg Chl | Monthly Avg Chl | Nodule Cover | Avg Temp | Avg Speed | Max Speed | Avg Current Direction |
|-------------|--------------|-------|----------|----------|-------|-----------------|-----------------|--------------|----------|-----------|-----------|-----------------------|
| | | (m) | 1:100 km | 50:250 m | | | | | | | | |
| DC1 | APEI7 AP | 4878 | -235 | -2 | 1.850 | 0.147 | 0.125 | 0.000 | 1.62 | 0.05 | 0.12 | 230.4 |
| DC2 | APEI7 AP | 4860 | -208 | -2 | 1.850 | 0.147 | 0.125 | 0.000 | 1.62 | 0.05 | 0.12 | 333.3 |
| DC3 | APEI7 S | 3083 | 903 | 44 | 1.973 | 0.147 | 0.124 | 0.000 | 1.8 | 0.06 | 0.14 | 328.2 |
| DC4 | APEI7 S | 3140 | 1345 | 12 | 2.014 | 0.147 | 0.124 | 0.000 | 1.79 | 0.08 | 0.18 | 29.7 |
| DC5 | APEI4 AP | 5216 | -217 | -16 | 1.380 | 0.117 | 0.119 | 0.526 | 1.67 | 0.09 | 0.13 | 176.1 |
| DC6 | APEI4 AP | 5004 | -138 | -2 | 1.430 | 0.117 | 0.120 | 0.148 | 1.64 | 0.08 | 0.14 | 1.3 |
| DC7 | APEI4 S | 3542 | 1098 | -36 | 1.327 | 0.116 | 0.108 | 0.000 | 1.68 | 0.05 | 0.15 | 27.3 |
| DC8 | APEI4 S | 3497 | 1310 | -9 | 1.428 | 0.116 | 0.106 | 0.000 | 1.7 | 0.04 | 0.16 | 129.5 |
| DC9 | APEI1 AP | 5236 | -81 | -10 | 1.105 | 0.073 | 0.062 | 0.142 | NA | NA | NA | NA |
| DC10 | APEI1 AP | 5213 | 25 | -18 | 1.156 | 0.073 | 0.063 | 0.099 | NA | NA | NA | NA |
| DC11 | APEI1 S | 4218 | 932 | -56 | 1.158 | 0.071 | 0.061 | 0.470 | NA | NA | NA | NA |
| DC12 | APEI1 S | 4346 | 831 | 4 | 1.118 | 0.072 | 0.063 | 0.738 | NA | NA | NA | NA |
| TC02 | APEI4 AP | 5096 | -150 | 17 | 1.430 | 0.117 | 0.120 | 0.000 | NA | NA | NA | NA |
| TC03 | APEI4 S | 3885 | 1201 | -22 | 1.327 | 0.115 | 0.106 | 0.000 | NA | NA | NA | NA |
| TC04 | APEI4 S | 4134 | 1218 | -2 | 1.355 | 0.115 | 0.106 | 0.000 | NA | NA | NA | NA |
| TC05 | APEI1 AP | 5225 | -46 | 27 | 1.105 | 0.073 | 0.062 | 0.299 | NA | NA | NA | NA |
| TC06 | APEI1 AP | 5249 | 14 | -10 | 1.156 | 0.073 | 0.063 | 0.079 | NA | NA | NA | NA |
| TC07 | APEI1 S | 4622 | 688 | -3 | 1.149 | 0.072 | 0.062 | 0.383 | NA | NA | NA | NA |

AP, abyssal plain; S, seamount.

gradient and any additional variability introduced with a change in latitude not accounted for by productivity/POC changes.

In addition to the PCoA analysis, PERMANOVA was used to evaluate how much the community composition was influenced by each available predictor, with the `adonis` function in the R package `{vegan}`. The permutations ($N = 9,999$) were again stratified by APEI. Significance was evaluated using marginal tests: PERMANOVA analyses were repeated so that each predictor could be evaluated as the last predictor added to the model, since the results depend on the order of the terms. Finally, in order to understand which animals were most responsible for driving differences between habitat types, a similarity percentages (SIMPER) analysis was conducted on the dissimilarity matrix using habitat type as the grouping variable (`simper` function in `{vegan}`). The eight taxa that represent >70% of the variation in community composition were considered the most significant taxa.

RESULTS

Seamounts vs. Plains: Environmental Characteristics

A total of 17 baited camera deployments and 5 baited trap deployments were conducted (Table 1, Note, DC7 was excluded due to bait consumption on descent). All deployment locations were on soft sediment. Nodule cover varied across the three APEIs, with no manganese nodules in APEI 7 deployments. APEI 4 was highly heterogeneous in nodule abundance with nodules covering 0 to 53% at abyssal locations (mean 13%; Table 2), and with no nodules observed in any of the four APEI 4 seamount deployments. All deployments in APEI 1, both on plains and seamounts, observed nodules, with the average percent coverage at 32% (8–74%). Across all sites, there were no clear relationships between nodule cover and habitat type.

For the eight deployments for which current meter data was available (APEI 7 and 4), seamount and abyssal plain deployments had similar mean current speeds around 0.06 m s^{-1} (seamount mean \pm sd $0.0575 \pm 0.02 \text{ m s}^{-1}$; plain mean \pm sd $0.0675 \pm 0.02 \text{ m s}^{-1}$; Table 2). Although seamounts average speeds were slightly lower than plains, this difference was not significant ($p = 0.65$). However, maximum recorded speeds were significantly higher on seamounts (0.15 m s^{-1}) than on abyssal plains (0.13 m s^{-1}). Seamount sediments were rippled, bright white, and much coarser than plain sediments in all APEIs, indicating bouts of active sediment transport and winnowing. Large gouge marks (>1 m in length), which may be some sort of feeding traces, were also visible in several seamount deployments.

Seamounts vs. Plains: Diversity

A total of 22 bait-attending taxa were identified across all 17 baited camera deployments (Figure 3 and Table 3). Twelve fish morphotaxa (family, genus, or species) were observed from six families, Synphobranchidae, Macrouridae, Ophidiidae, Alepocephalidae, Halosauridae, Zoarcidae. Seven crustacean morphotaxa were also observed including a squat lobster (*Munidopsis* sp.) and several types of shrimps (Period, Aristeid,

and Caridean shrimps). Additionally, one genus of octopus was observed, *Grimpoteuthis* sp. Finally, bait-attending echinoderms were represented by the brittle star *Ophiophalma* cf. *glabrum*, and an unidentified echinoid. At the APEI 7 seamount (DC3). One deployment (DC7) was not considered in the statistical analysis because shallow-water sharks ate nearly all of the bait before the lander reached bottom, leaving the deployment with some bait scent, but essentially un-baited for the entire duration. Fifteen taxa were observed across the abyssal plain deployments, and 22 taxa were observed across the seamount deployments.

Rarified diversity showed that seamounts have significantly higher morphospecies richness ($q = 0$) than plains (Figure 4B), and morphospecies accumulation curves suggest that while abyssal plains seem to have been sufficiently sampled, seamount richness has not yet reached an asymptote (Figure 4A). Extrapolated morphospecies richness at 614 individuals was calculated to be 15.4, [standard error (se) = 2.7] for abyssal plains and 22.3 (se = 3.9) for seamounts, and CI were non-overlapping by 450 individuals. For both Shannon and Simpson diversity metrics ($q = 1,2$), seamounts were significantly less diverse than abyssal plains (Figures 4C,D). This is due to low evenness scores on seamounts, driven by the extremely high abundances of the predator and scavenger *I. arx*, identified to species from baited-trap specimens (Leitner et al., 2020; Table 3).

Comparisons between APEIs (with habitat types combined within each APEI) showed no significant differences in morphospecies richness ($q = 0$) among APEIs, but significantly lower Shannon and Simpson diversities ($q = 1,2$) in APEI 7 (Figures 5B–D). The diversity metrics were lower in APEI 7 due to the extreme dominance of *I. arx* on the APEI 7 seamount, with MaxN for *I. arx* an order of magnitude greater than for all other morphospecies. Morphospecies accumulation curves for each APEI indicate that only APEI 4 approached an asymptote, suggesting that more morphospecies are likely to be found upon further sampling in APEI 1 and 7 (Figure 5A).

Seamounts vs. Plains: Taxonomic Overlap

Seven morphospecies were only found on seamounts, including the most abundant bait-attending taxon observed, the synphobranchid eel *I. arx* (MaxN = 115). *Ilyophis arx* dominated scavenger abundance and was responsible for the vast majority of the bait consumption on seamounts in APEI 7 and 4. Four morphotaxa (*Asquamiceps*, Halosaur, *Bassogigas walkeri*, and Zoarcidae sp. 2) were unique to the seamount in APEI 7. One morphotaxon (echinoid) was unique to the seamount in APEI 4. The seamount in APEI 1 had no exclusive morphotaxa but shared one morphotaxon (*Acanthephyra* sp.) exclusively with the seamount in APEI 7. No bait-attending morphotaxon was exclusively found on abyssal plains. The greatest amount of morphospecies overlap ($N = 6$) was found between all sites except APEI 7 seamount, which was clearly the most distinct site (Figure 6 and Table 4). Only two taxa were common to all sites, the ophidiid *Bassozetus* sp. B, and the summed taxonomic category of large penaeid and aristeid shrimps (a category used when distinguishing characteristics like rostrum length and

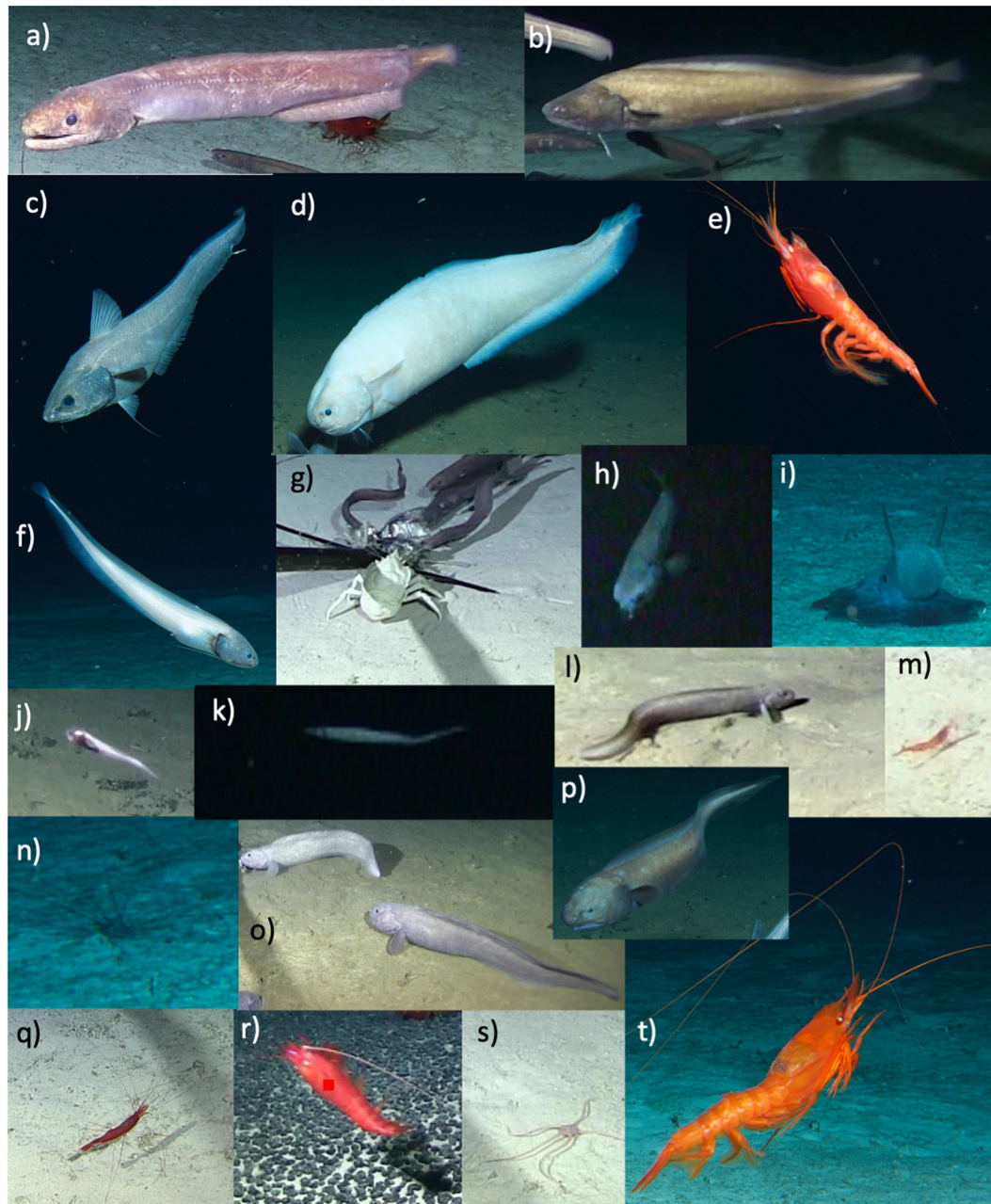


FIGURE 3 | Twentymorphospecies seen across the seventeen successful baited camera deployments. **(a)** *Ilyophis arx* **(b)** *Bassogigas walkeri* **(c)** *Coryphaenoides armatus/yaquinae* complex **(d)** *Barathrites iris* **(e)** *Benthiscymus* sp. **(f)** *Bassozetus* sp. B **(g)** *Munidopsis* sp. **(h)** *Asquamiceps* sp. **(i)** *Grimpoteuthis* sp. **(j)** *Bassozetus* juvenile sp. **(k)** Halosaur **(l)** Zoarcid sp. 2 **(m)** *Hymenopenaeus nereus* **(n)** Echinoid **(o)** *Pachycara nazca* **(p)** *Bassozetus nasus* **(q)** *Nematocarcinus* sp. **(r)** *Acanthephyra* sp. **(s)** *Ophiosphalma* c.f. *glabrum* **(t)** *Cerataspis monstrosus*.

shape were not visible to distinguish *Cerataspis monstrosus* from *Benthiscymus* sp.).

Seamounts vs. Plains: Community Composition

Seamounts have significantly different community compositions than plains (PERMANOVA $p < 0.001$). From the SIMPER

analysis, the eight morphotaxa most influential in driving the differences between seamount and abyssal plain communities were the synbranchid eel *I. arx* (21% of the difference), the abyssal rattail *Coryphaenoides armatus/yaquinae* (12%), large decapod shrimp (as a general taxonomic category, 9%), the shrimp morphospecies *C. monstrosus* (7%), the ophiidiid *Barathrites iris* (6%), the zoarcid *Pachycara nazca* (6%), and two ophiidiids: juvenile *Bassozetus* sp. (5%) and *Bassozetus* sp. B (5%).

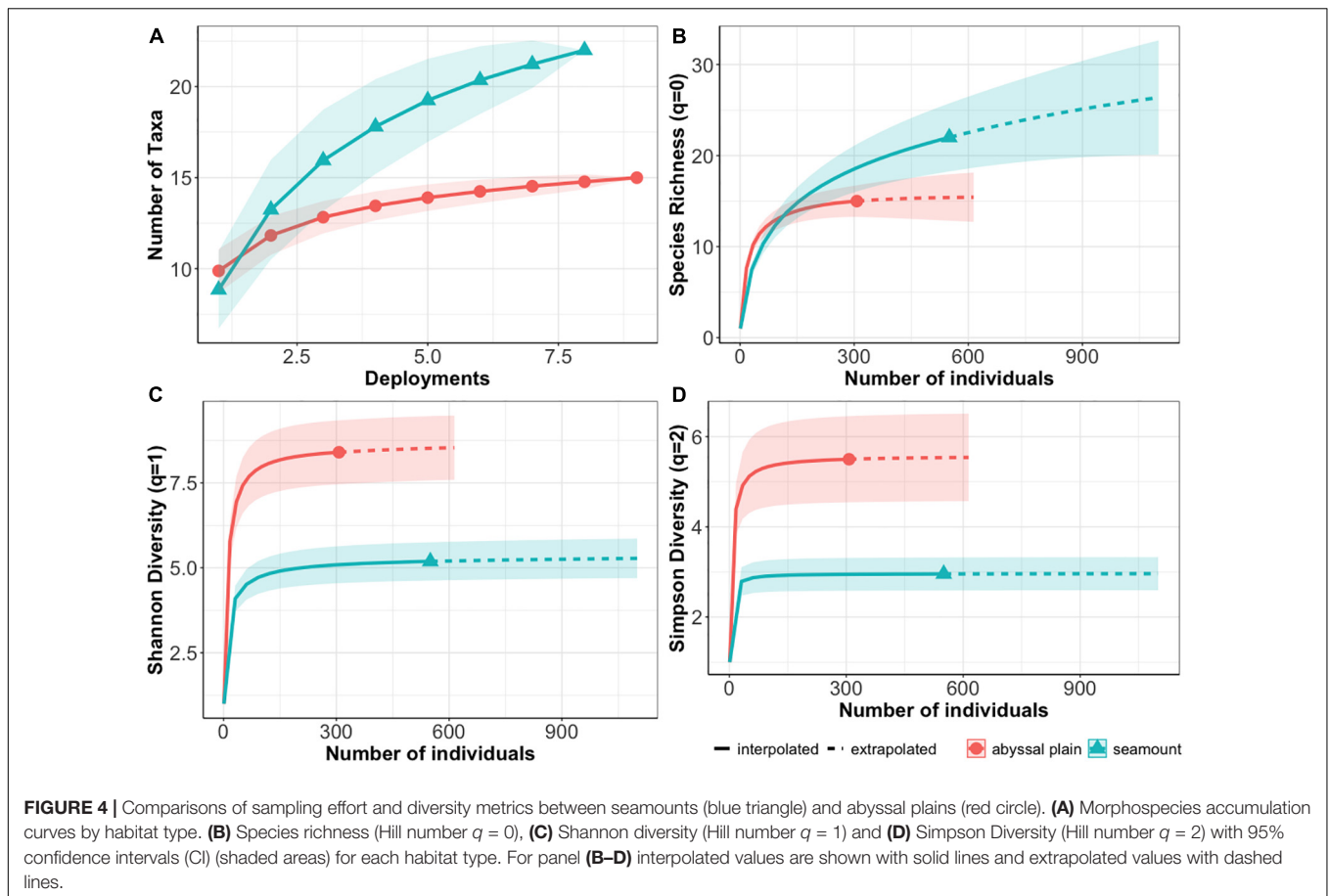
TABLE 3 | (A) Relative abundances (MaxN) of all bait-attending fishes in all successful deployments. (B) Relative abundances (MaxN) of all bait-attending invertebrate fauna in all successful deployments.**(A)**

| Station name | Drop | <i>Asquamiceps</i> sp. | Halosaur | <i>Coryphaenoides armatus/ yaquinae</i> | <i>Barathrites iris</i> | <i>Bassogigas walkeri</i> | <i>Bassozetus nasus</i> | <i>Bassozetus</i> spp | <i>Bassozetus</i> sp.B | <i>Bassozetus</i> sp. juv | <i>Ilyophis arx</i> | <i>Pachycara nazca</i> | <i>Zoarcidae</i> sp.2 |
|--------------|-------------|------------------------|----------|---|-------------------------|---------------------------|-------------------------|-----------------------|------------------------|---------------------------|---------------------|------------------------|-----------------------|
| APEI7 AP | DC1 | 0 | 0 | 20 | 2 | 0 | 1 | 0 | 0 | 0 | 0 | 3 | 0 |
| APEI7 AP | DC2 | 0 | 0 | 21 | 2 | 0 | 0 | 0 | 1 | 0 | 0 | 2 | 0 |
| APEI7 S | DC3 | 1 | 0 | 0 | 0 | 2 | 0 | 0 | 2 | 0 | 115 | 0 | 1 |
| APEI7 S | DC4 | 0 | 1 | 0 | 0 | 2 | 0 | 1 | 2 | 0 | 110 | 0 | 2 |
| APEI4 AP | DC5 | 0 | 0 | 10 | 2 | 0 | 4 | 0 | 1 | 3 | 0 | 0 | 0 |
| APEI4 AP | DC6 | 0 | 0 | 20 | 1 | 0 | 1 | 0 | 1 | 1 | 0 | 8 | 0 |
| APEI4 S | DC7 | 0 | 0 | 0 | 0 | 0 | 0 | 0 | 1 | 0 | 4 | 0 | 0 |
| APEI4 S | DC8 | 0 | 0 | 3 | 0 | 0 | 1 | 0 | 2 | 0 | 56 | 8 | 0 |
| APEI1 AP | DC9 | 0 | 0 | 15 | 2 | 0 | 2 | 0 | 0 | 2 | 0 | 0 | 0 |
| APEI1 AP | DC10 | 0 | 0 | 8 | 2 | 0 | 2 | 3 | 1 | 5 | 0 | 0 | 0 |
| APEI1 S | DC11 | 0 | 0 | 2 | 0 | 0 | 2 | 0 | 0 | 0 | 1 | 0 | 0 |
| APEI1 S | DC12 | 0 | 0 | 3 | 0 | 0 | 2 | 0 | 1 | 0 | 0 | 0 | 0 |
| APEI4 AP | TC02 | 0 | 0 | 11 | 4 | 0 | 2 | 0 | 1 | 0 | 0 | 9 | 0 |
| APEI4 S | TC03 | 0 | 0 | 0 | 1 | 0 | 2 | 0 | 6 | 1 | 15 | 1 | 0 |
| APEI4 S | TC04 | 0 | 0 | 1 | 1 | 0 | 7 | 0 | 5 | 5 | 3 | 1 | 0 |
| APEI1 AP | TC05 | 0 | 0 | 5 | 5 | 0 | 3 | 0 | 0 | 4 | 0 | 1 | 0 |
| APEI1 AP | TC06 | 0 | 0 | 4 | 1 | 0 | 3 | 0 | 1 | 4 | 0 | 0 | 0 |
| APEI1 S | TC07 | 0 | 0 | 3 | 0 | 0 | 2 | 0 | 0 | 1 | 0 | 0 | 0 |

TABLE 3 | Continued

(B)

| Station Name | Drop | <i>Munidopsis</i> sp. | <i>Acanthephyra</i> sp. | total shrimp Penaeid /Aristeidae | <i>Cerataspis monstrosus</i> | <i>Benthiscymus</i> sp | <i>Hymenop- enaeus nereus</i> | <i>Nemato- carcinus</i> sp | <i>Grimpoteuthis</i> sp | <i>Echinoidea</i> | <i>Ophiosphalma glabrum</i> |
|--------------|------|-----------------------|-------------------------|----------------------------------|------------------------------|------------------------|-------------------------------|----------------------------|-------------------------|-------------------|-----------------------------|
| APEI7 AP | DC1 | 0 | 0 | 3 | 3 | 2 | 1 | 0 | 0 | 0 | 0 |
| APEI7 AP | DC2 | 1 | 0 | 0 | 2 | 2 | 1 | 1 | 0 | 0 | 0 |
| APEI7 S | DC3 | 0 | 1 | 1 | 0 | 0 | 0 | 0 | 0 | 0 | 0 |
| APEI7 S | DC4 | 1 | 1 | 1 | 0 | 0 | 0 | 0 | 0 | 0 | 1 |
| APEI4 AP | DC5 | 0 | 0 | 5 | 3 | 2 | 1 | 0 | 1 | 0 | 1 |
| APEI4 AP | DC6 | 0 | 0 | 3 | 3 | 1 | 1 | 0 | 1 | 0 | 0 |
| APEI4 S | DC7 | 0 | 0 | 2 | 1 | 1 | 0 | 0 | 0 | 0 | 0 |
| APEI4 S | DC8 | 0 | 0 | 7 | 5 | 0 | 0 | 0 | 0 | 0 | 0 |
| APEI1 AP | DC9 | 0 | 0 | 4 | 1 | 2 | 1 | 0 | 0 | 0 | 0 |
| APEI1 AP | DC10 | 0 | 0 | 6 | 3 | 3 | 1 | 0 | 0 | 0 | 2 |
| APEI1 S | DC11 | 0 | 0 | 23 | 23 | 1 | 1 | 0 | 0 | 0 | 0 |
| APEI1 S | DC12 | 0 | 1 | 11 | 5 | 1 | 0 | 0 | 0 | 0 | 0 |
| APEI4 AP | TC02 | 0 | 0 | 5 | 4 | 2 | 1 | 1 | 0 | 0 | 1 |
| APEI4 S | TC03 | 0 | 0 | 14 | 9 | 1 | 0 | 1 | 0 | 1 | 0 |
| APEI4 S | TC04 | 0 | 0 | 12 | 9 | 2 | 1 | 1 | 1 | 0 | 0 |
| APEI1 AP | TC05 | 0 | 0 | 3 | 3 | 2 | 2 | 0 | 0 | 0 | 3 |
| APEI1 AP | TC06 | 0 | 0 | 7 | 3 | 3 | 1 | 1 | 0 | 0 | 0 |
| APEI1 S | TC07 | 0 | 0 | 18 | 10 | 2 | 7 | 1 | 1 | 0 | 0 |



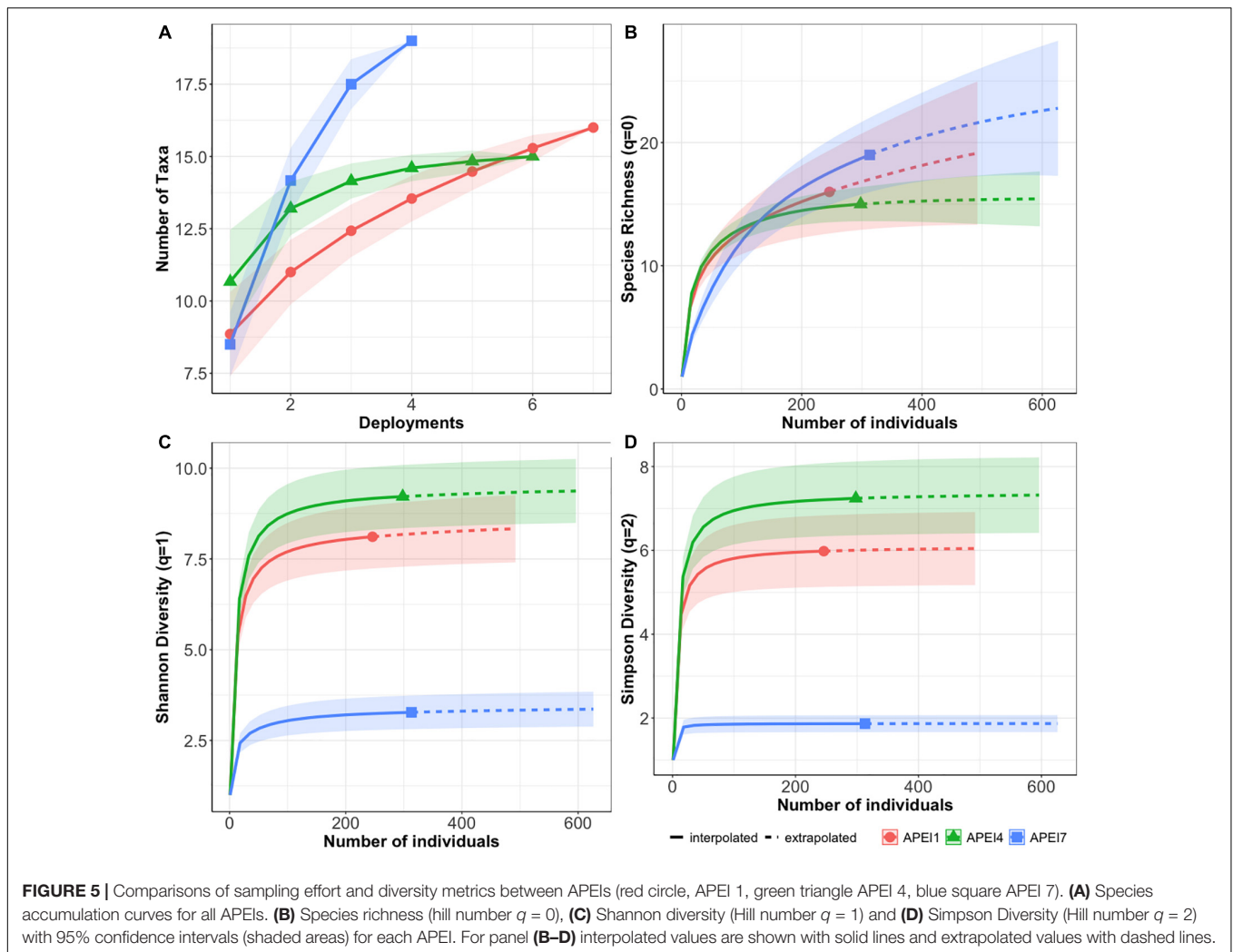
The three APEIs also had significantly different community compositions (PERMANOVA $p < 0.05$), and *I. arx* was always the most influential taxa in driving the differences in community compositions in the areas. Over one quarter of the differences between each APEI pair is explained by the relative abundances of *I. arx* and *C. armatus/yaquinae*; though for the APEI 1 and 4 pair, *P. nazca* (12%) accounts for more variation than *C. armatus/yaquinae* (10%).

Of the environmental predictors analyzed, marginal significance tests consistently found that BBPI (habitat type), latitude, and POC flux had significant influences on relative abundances and community composition ($p < 0.05$). Lander type did not have a significant effect. The constrained ordination with these predictors as well as with nodule abundance and lander type (not significant) was able to explain 69% of the variability in the community compositions across the deployments (Figure 7). The first two ordination axes alone explained 61% of the variation.

Cluster analysis (simprof) found eight significant clusters of deployments, and no seamount deployments clustered with any abyssal plain deployments (Figure 7 and Supplementary Figure 1). Deployments from the two different landers, DC and Tripod, were never included in the same significant clusters; however, marginal tests found that lander type did not significantly affect the community composition ($p > 0.05$). The

APEI 7 seamount deployments formed their own significant, unique cluster. These two deployments were part of another cluster with the only successful DC deployment on the APEI 4 seamount. These three seamount deployments were all marked by high abundances of *I. arx* (Leitner et al., 2021). Both Tripod deployments on the APEI 4 seamount cluster together, though separately from one the DC deployment on that same seamount. Likewise, both DC deployments on the APEI 1 seamount cluster together, while the only tripod deployment on the APEI 1 seamount was in a separate cluster on its own. Abyssal plain communities were more similar to each other than to those at their proximate seamounts, as evidenced by the cluster analysis. Seamounts host distinct communities from plains, though the differences decrease with increasing latitude such that the seamounts in APEI 1 were the closest in composition to that of the plains. Abyssal plain deployments seem to be grouped by APEI; though APEI 4 plain deployments showed a transitional community, with one deployment grouping with the APEI 1 plain cluster and the others with the APEI 7 plain cluster (Figure 7 and Supplementary Figure 1).

While the abyssal seamounts sampled here generally had higher overall relative abundances (MaxN) than the surrounding abyssal plains, this “seamount-effect” was highly taxon-specific, with some animals found at significantly higher abundances

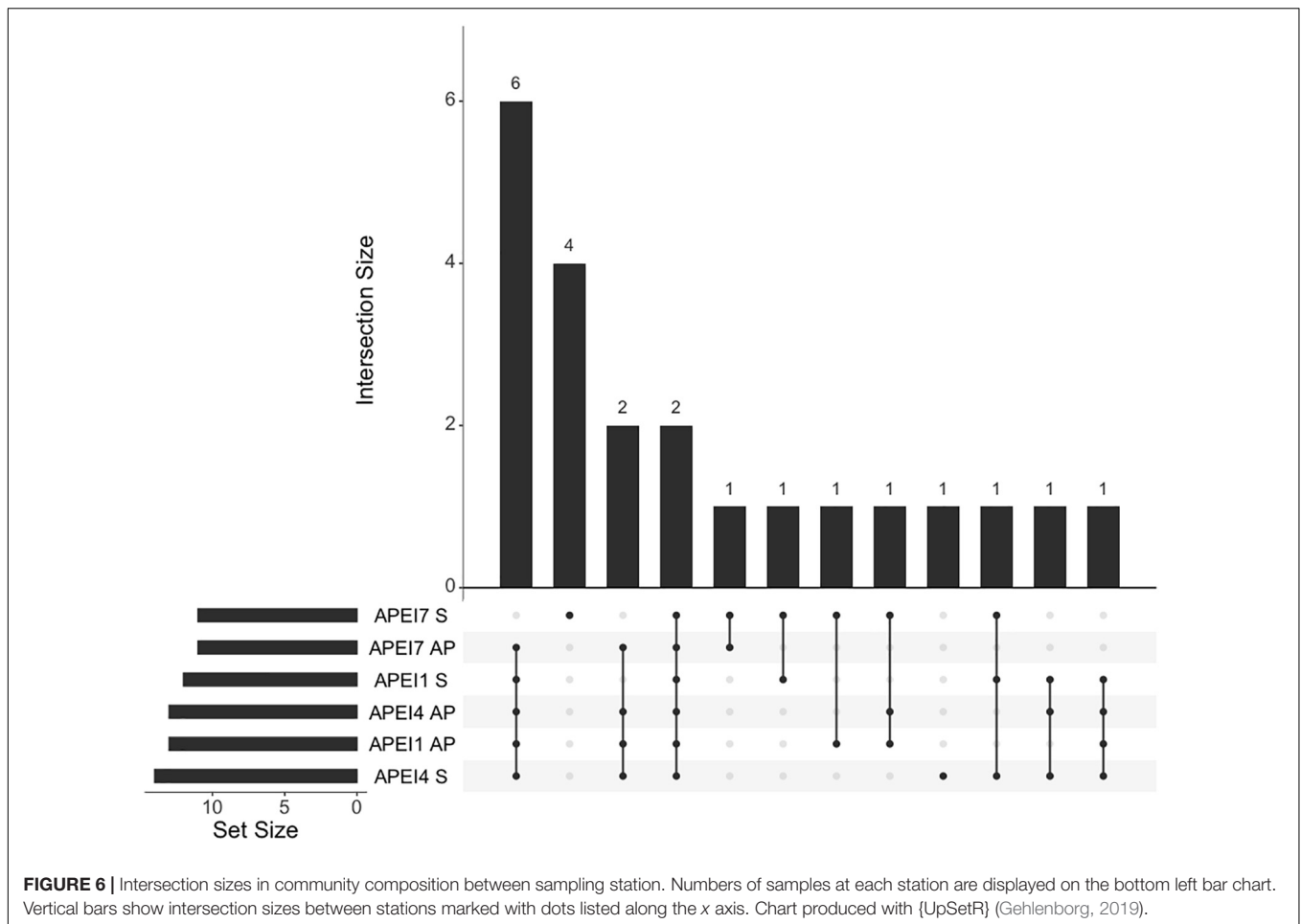


on seamounts and others on abyssal plains. The abyssal plain communities were distinguished by higher abundances of *C. armatus/yaquinae*, *B. iris*, juvenile *Bassozetus* sp., *P. nazca*, *Benthiscymus* sp., and *O. glabrum*. The abyssal seamount communities were distinguished by higher abundances of *Larx*, *Bassozetus* sp. B, *B. walkeri*, total shrimp, and *C. monstrosus* (Figure 8).

DISCUSSION

The main goals of this study were to describe the bait-attending assemblage from abyssal seamounts for the first time and to test the “shared-fauna” prediction of the SRH in the western CCZ in the context of deep-sea mining for bait-attending abyssal-demersal fauna. These are mid-level and top predators, necrophagivores, and scavengers in abyssal seafloor ecosystems. From our observations, we cannot reject the SRH for the bait-attending community. All abyssal plain morphospecies were also seen on at least one seamount deployment. However, the reverse was not true. In fact, seven morphospecies were exclusive to

seamount deployments. Therefore, these abyssal seamounts were found to host diverse and different bait-attending assemblages in comparison to their neighboring abyssal plains. In fact, abyssal plain assemblages hundreds of kilometers apart were more similar to each other, than to those assemblages on seamounts just 15 km away. The seamounts sampled also had different dominant fauna, with synphobranchid eels dominating in the southern two seamounts, and large decapod shrimps dominating the community in the northern seamount. The significant differences in community structure make it unlikely that displaced animals will venture up into the seamount habitat in sufficient numbers to create and sustain viable populations on the timescales required for recovery (>26 years), even to avoid negative mining impacts such as extensive sediment plumes and reduction or elimination of infaunal and benthic prey (Gollner et al., 2017; Jones et al., 2017; Simon-Lledó et al., 2019). While highly mobile animals are often found in a variety of habitats, their core habitat, where they are naturally the most abundant, is often needed to sustain reproductive populations (Drazen et al., 2019). Moreover, seamounts make up only 0.3% of the habitat area of the CCZ (Washburn et al., 2021) and ecological research shows that a 99%



habitat loss results in extinctions of essentially all species reliant on that habitat (Hanski et al., 2013; Rybicki and Hanski, 2013). Thus, protection of seamounts in the CCZ region alone does not appear to be sufficient to preserve abyssal biodiversity, even if all the mobile abyssal species can live on seamounts. Therefore, while we found no morphospecies exclusive to abyssal plains, we argue that distinct differences in densities indicate that only preserving seamounts is likely to be insufficient refuge for top predators and scavengers of the CCZ.

Often, seamounts are considered unusual habitats in the deep-sea because they provide hard substrate, which can be rare in much of the deep sea (but see Riehl et al., 2020; Smith et al., 2020). Previous works comparing seamounts to surrounding abyssal plains face two complications. Firstly, these studies mostly attempted to compare fauna at bathyal depths on seamounts to fauna at abyssal depths on plains (e.g., Christiansen et al., 2015; Vieira et al., 2018), so any difference between seamounts and abyssal plains may result from the strong vertical zonation of fauna across this depth gradient (Christiansen et al., 2015; Denda et al., 2017; Linley et al., 2017) instead of geomorphology. Secondly, most studies compared hard-substrate habitats, which predominate on seamounts, to soft-substrate plain habitats, making it difficult to distinguish a seamount effect from a

substrate effect (e.g., Christiansen et al., 2015; Vieira et al., 2018). Here we specifically compared soft-sediment habitats on abyssal seamounts to surrounding soft-sediment abyssal plains, making the clear community differences between seamounts and abyssal plains reported particularly noteworthy, especially because bait-attending fauna are mobile and generally widespread. One study in the Atlantic abyssal plains for example, showed no difference in the fish communities between abyssal plains and abyssal highs with elevations less than 1,000 m (Milligan et al., 2016). However, for the same area, abyssal hills were found to have significantly higher biomass, higher diversity, and a different trophic composition for the invertebrate, benthic megafaunal community (Durden et al., 2015). Moreover, across a gradient of low relief bathymetric change within the CCZ, another study found significantly higher abundances, larger body sizes, higher diversity, and different community composition for bait-attending fauna at higher relative elevations (abyssal hills) vs. plains and depressions (Leitner et al., 2017). Finally, a recent study has found that even changes in depth as small as 10s of meters can significantly influence the benthic megafaunal community (Durden et al., 2020). Thus, a bathymetric change of 1,000 m, even without a substrate change, would be expected to affect the megafaunal community.

TABLE 4 | Presence table for each bait-attending taxon in order of most widely observed.

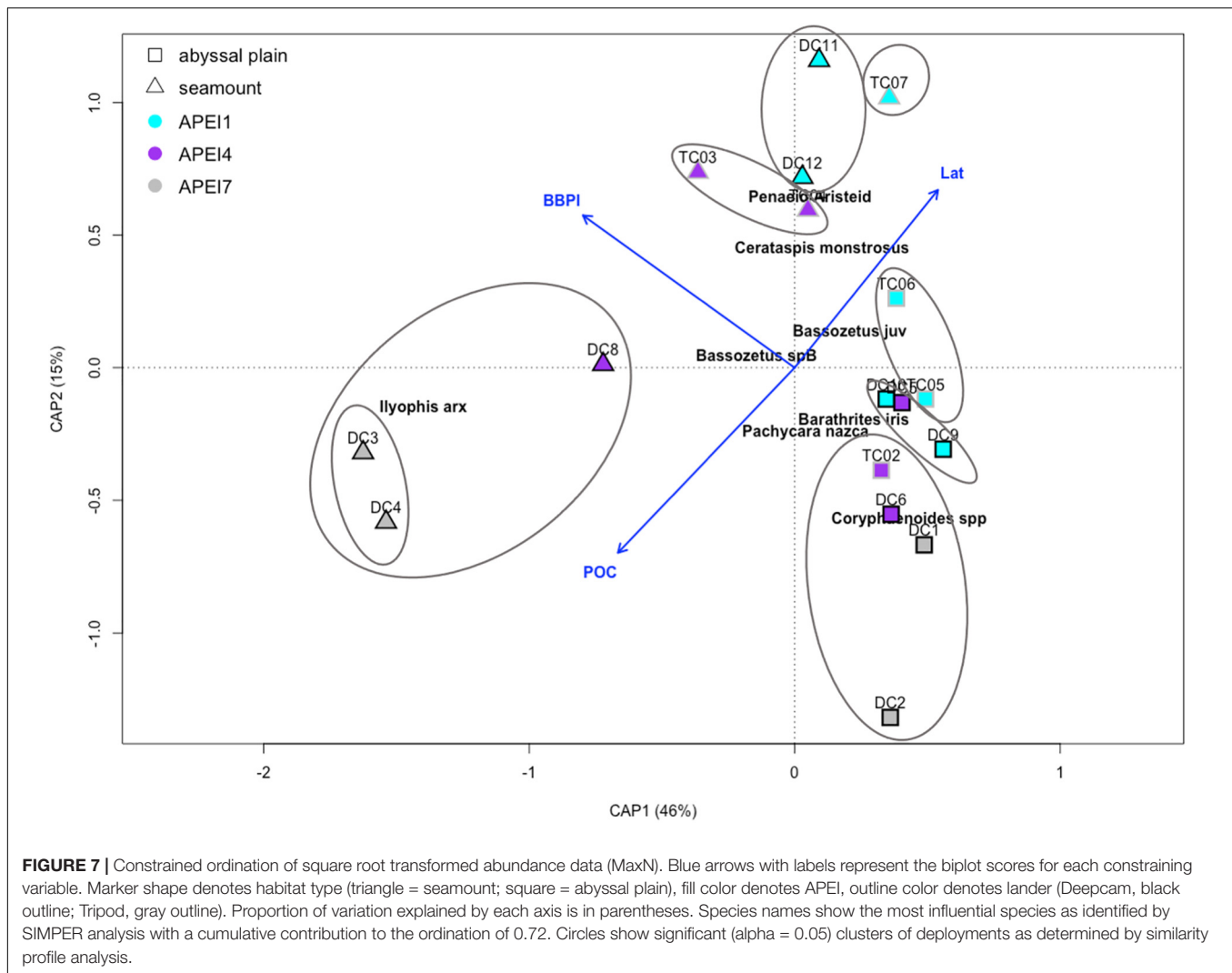
| Taxon | Total N sites | APEI1 AP | APEI1 S | APEI4 AP | APEI4 S | APEI7 AP | APEI7 S | SM | AP |
|--|---------------|----------|----------|----------|----------|----------|----------|----|----|
| <i>Bassozetus</i> spB | 6 | 1 | 1 | 1 | 1 | 1 | 1 | 3 | 3 |
| Total Shrimp Penaeidae/Aristeidae | 6 | 1 | 1 | 1 | 1 | 1 | 1 | 3 | 3 |
| <i>Coryphaenoides armatus/yaquinae</i> | 5 | 1 | 1 | 1 | 1 | 1 | 0 | 2 | 3 |
| <i>Bassozetus nasus</i> | 5 | 1 | 1 | 1 | 1 | 1 | 0 | 2 | 3 |
| <i>Cerataspis monstrosus</i> | 5 | 1 | 1 | 1 | 1 | 1 | 0 | 2 | 3 |
| <i>Benthiscymus</i> sp. | 5 | 1 | 1 | 1 | 1 | 1 | 0 | 2 | 3 |
| <i>Hymenopenaeus nereus</i> | 5 | 1 | 1 | 1 | 1 | 1 | 0 | 2 | 3 |
| <i>Nematocarcinus</i> sp. | 5 | 1 | 1 | 1 | 1 | 1 | 0 | 2 | 3 |
| <i>Barathrites iris</i> | 4 | 1 | 0 | 1 | 1 | 1 | 0 | 1 | 3 |
| <i>Bassozetus</i> sp. juv | 4 | 1 | 1 | 1 | 1 | 0 | 0 | 2 | 2 |
| <i>Pachycara nazca</i> | 4 | 1 | 0 | 1 | 1 | 1 | 0 | 1 | 3 |
| <i>Ilyophis arx</i> | 3 | 0 | 1 | 0 | 1 | 0 | 1 | 3 | 0 |
| <i>Grimpoteuthis</i> sp. | 3 | 0 | 1 | 1 | 1 | 0 | 0 | 2 | 1 |
| <i>Ophiosphalma glabrum</i> | 3 | 1 | 0 | 1 | 0 | 0 | 1 | 1 | 2 |
| <i>Bassozetus</i> spp. | 2 | 1 | 0 | 0 | 0 | 0 | 1 | 1 | 1 |
| <i>Munidopsis</i> sp. | 2 | 0 | 0 | 0 | 0 | 1 | 1 | 1 | 1 |
| <i>Acanthephyra</i> sp. | 2 | 0 | 1 | 0 | 0 | 0 | 1 | 2 | 0 |
| <i>Asquamiceps</i> | 1 | 0 | 0 | 0 | 0 | 0 | 1 | 1 | 0 |
| Halosaur | 1 | 0 | 0 | 0 | 0 | 0 | 1 | 1 | 0 |
| <i>Bassogigas walkeri</i> | 1 | 0 | 0 | 0 | 0 | 0 | 1 | 1 | 0 |
| Zoarcidae sp.2 | 1 | 0 | 0 | 0 | 0 | 0 | 1 | 1 | 0 |
| Echinoidea | 1 | 0 | 0 | 0 | 1 | 0 | 0 | 1 | 0 |

The first column displays the number of sites (APEI and habitat type combinations, $N = 6$) where each taxon was observed at least once. The middle columns show presence (1) or absence (0) at each site. The last two columns show the number of sites where each taxon was observed at least once split by habitat type, SM, seamount; AP, abyssal plain. Gray fill color highlights seamount exclusive taxa. Bolded 1 values represent present, plain text 0s represent absences.

Cuvelier et al. (2020) and Laroche et al. (2020) conducted the only other tests of the SRH in the CCZ, and their results differ from ours in finding lower taxonomic overlap between seamounts and abyssal plains than reported here for bait-attending fauna. Cuvelier et al. (2020) used ROV video and compared the megafaunal communities, excluding fishes, of four seamounts and surrounding nodule fields and found, similar to the results here, that seamounts hosted distinct benthic megafaunal communities. However, they found only 10% taxonomic overlap between abyssal plains and seamounts. Laroche et al. (2020) also found that abyssal seamounts and neighboring abyssal-plain communities (the same locations studied here) were distinct based on eDNA sampling of sediment and bottom waters, finding only 16–19% seamount vs. plain overlap in amplicon sequence variants. Both studies concluded that the SRH was not valid for mining impacts in the CCZ due to low degrees of faunal overlap (Cuvelier et al., 2020). While we did find 7 of 22 morphospecies unique to the sampled seamounts, we found much higher (68%) taxonomic overlap between seamounts and plains. Moreover, all of the abyssal bait-attending morphospecies were also found on seamounts, though often in much lower numbers. Thus, seamounts may provide better refugia for the highly mobile scavengers/predators than for the much less mobile megafaunal deposit and suspension feeders. It should be noted that while Cuvelier et al. (2020) did have data from abyssal depths on three of the visited seamounts, all but one of their seamounts extended into bathyal depths, making these

bathyal seamounts rather than the abyssal seamounts as discussed here. In addition, fishes were left out of their comparative statistical analysis due to their lack of representativity and possibly attraction to the ROV lights, although the authors did report greater fish diversity on seamounts than in abyssal nodule fields (Cuvelier et al., 2020). Laroche et al. (2020) found that fishes represented only a small fraction of the amplicon sequence variants identified, making seamount vs. abyssal-plain comparisons difficult.

Studies from bathyal seamounts in other regions, though shallower than the present work, show some similarities to our findings. Witte (1999) reported results from a large carcass experiment on a bathyal seamount summit (1,900 m depth) in the Arabian sea. High numbers of large aristeid shrimps were recorded at the bait, similar to our observations at the seamount in APEI 1. However, Witte also found a high number of macrourids at the bathyal seamount summit, which were absent at the nearby abyssal plain site, which was instead dominated by scavenging amphipods and large numbers of zoarcid fishes (Witte, 1999). Nevertheless, similar to our findings here, Witte found a distinct scavenging community at the seamount summit, though the dominant seamount taxa were different from those we found in the western CCZ. The only other baited camera data available from deep, oceanic seamounts come from Wilson et al. (1985), who studied the bait-attending community of one bathyal seamount (1,443 m) in the North Pacific. They observed halosaurs and shrimp from the genus *Acanthephyra*,

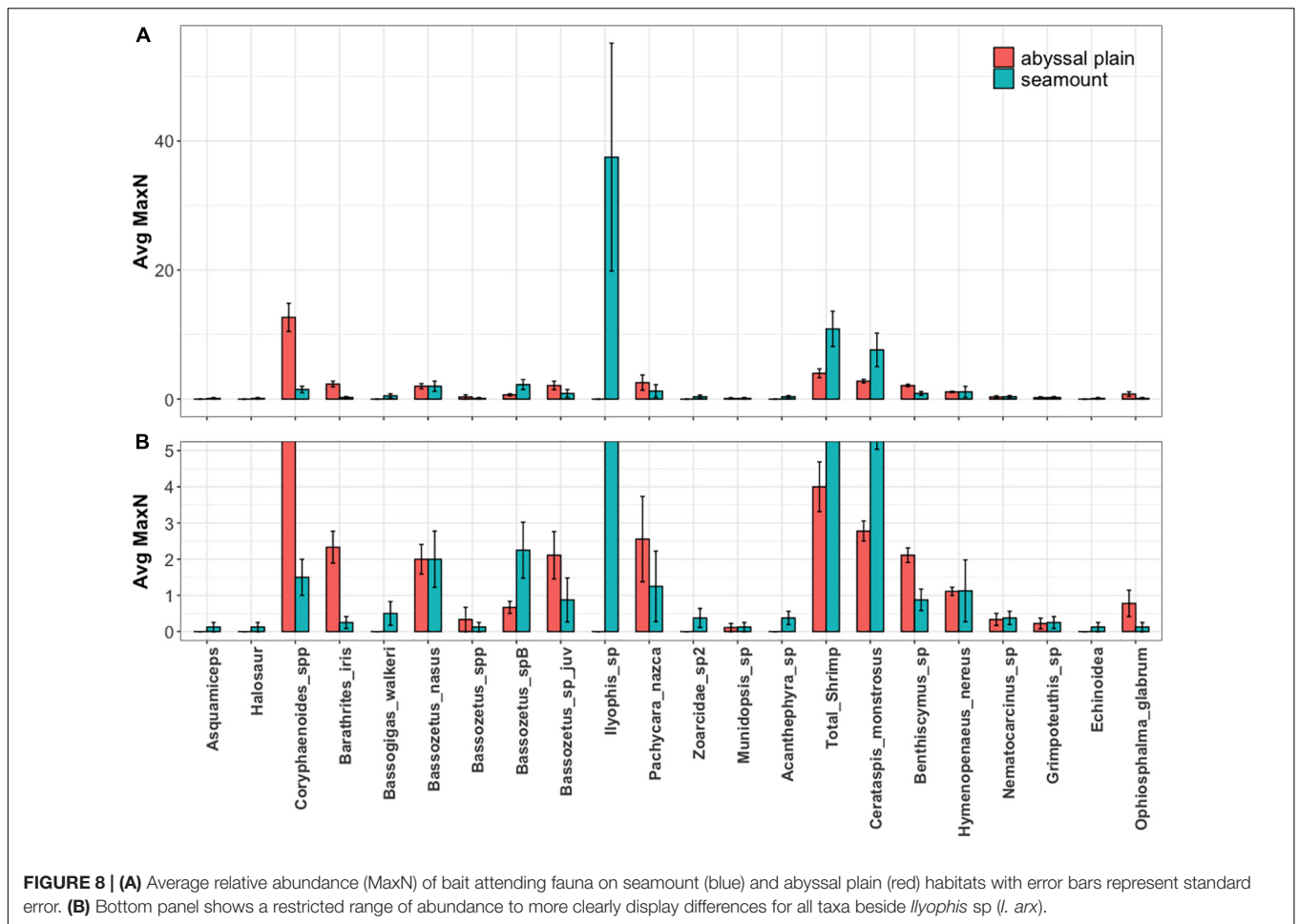


which we find to be seamount-associated and absent from the proximate abyssal plains. Wilson et al. (1985) also observed high numbers of penaeid shrimp around the bait, as well as several morphospecies of synphobranchid eels, though none in high numbers (MaxN = 4). Our results are also consistent with a study on the shallow Ampere Seamount in the NE Atlantic by Christiansen et al. (2015), who found large numbers of synphobranchid eels on the bathyal slopes of the seamount. In this study only a single species (an alepocephalid) was shared between the deep slopes of Ampere seamount and the abyssal reference site.

Despite the fact that small abyssal seamounts (seamounts whose summit depths are $\geq 3,000$ m) are the most common class of seamounts (Wessel et al., 2010), they are some of the most understudied, least explored habitats in the deep sea. The deployments discussed here, to our knowledge, yielded the first baited camera data published from abyssal seamounts. To date, seamount research has generally focused on shallower seamounts, which can be productivity hotspots, with abundant, high biomass, and diverse pelagic and benthic communities

(Holland and Grubbs, 2007; Pitcher et al., 2007; Morato et al., 2010; Rowden et al., 2010; Leitner et al., 2020). This “seamount effect” is still not fully understood, but is likely due to the added habitat heterogeneity provided by the seamount structure and increased food availability due to modified hydrodynamics and topographic blocking of mesopelagic migrators (Genin et al., 1988; Genin, 2004; Genin and Dower, 2007; Morato et al., 2009; Lavelle and Mohn, 2010). Whether this “seamount effect” extends to the deepest, and most ubiquitous seamounts in the global ocean, remains uncertain, mostly due to the lack of data from deep features (Wilson et al., 1985; Wessel, 2001; Rowden et al., 2010). Evidence from abyssal hills suggest that such seamount effects may extend to the abyss, since abyssal hills can have higher detrital food availability (Morris et al., 2016; Durden et al., 2017).

Our observations provide initial evidence that this “seamount effect” can apply to abyssal seamounts in some cases. Seamounts in the western CCZ hosted higher community relative abundances than the proximate abyssal plains and had higher morphospecies richness. Moreover, our analysis showed that there are likely more as of yet unrecorded taxa on seamounts.



Higher order diversity metrics showed that seamount diversity was lower than abyssal plain diversity, though this was due to low evenness, not to low richness. The extraordinarily high relative abundances of eels (in APEI 4 and 7) and shrimps (APEI 1) on these seamounts resulted in lower Shannon and Simpson diversity estimates. It must also be noted that the individual seamounts themselves had distinct communities, with each feature in each of the APEIs clustering separately. Therefore, while the communities on the three sampled seamounts were more similar to each other than to those on the surrounding plains, each seamount also had a unique community. Therefore, these abyssal seamounts enhance regional biodiversity, though the mechanisms are not yet fully clear. POC flux, a proxy for food availability in the deep-sea, was found to be a significant driver of differences in community composition (in addition to BBPI/habitat type). More sampling should be conducted on abyssal seamounts, especially on those within high productivity regimes, to examine further the relationship found here between high relative abundances on seamounts as well as high single taxon dominance and productivity.

Currently, community and diversity analyses are hampered by limited taxonomic resolution. While baited cameras are an efficient and unobtrusive method for observing abyssal fishes,

scavengers, and predators, physical sampling through trawls and additional traps are important complementary sampling methods that would enable additional species level identifications (Drazen and Sutton, 2017; Priede, 2017; Drazen et al., 2021, this vol). This information is currently lacking for many megafaunal species in the CCZ, because there has been no trawling in this area. Nevertheless, ISA-mandated environmental baselines require detailed taxonomic resolution in order to be effective (Wedding et al., 2015; Smith et al., 2020). Thus, there is a need for additional complementary physical sampling at this stage.

Our results show that abyssal seamounts host distinct, morphospecies-rich, communities that contribute to the regional biodiversity of the CCZ. These seamounts may not face direct mining impacts due to their challenging terrain but, it must not be assumed that because CCZ seamounts will not face manganese nodule mining, that they will not be impacted by mining activities. Nodule extraction on abyssal plains will likely generate large sediment plumes, both at the seafloor and in the midwater, that potentially could spread over 100s of kilometers (Drazen et al., 2020; Smith et al., 2020). Nearby seamount habitats therefore could also sustain impacts from these sediment plumes. Therefore, these distinct habitats merit consideration for environmental protection and further scientific study.

DATA AVAILABILITY STATEMENT

The original contributions presented in the study are included in the article/**Supplementary Material**, further inquiries can be directed to the corresponding author/s.

ETHICS STATEMENT

Ethical review and approval was not required for the animal study because this was a non-extractive video study.

AUTHOR CONTRIBUTIONS

AL, JD, and CS conceived of the project and conducted the field work, interpreted the results and drew final conclusions. AL annotated the video data, conducted statistical analyses, and wrote the body of the manuscript. JD and CS edited and made substantial contributions to the manuscript writing. All authors contributed to the article and approved the submitted version.

FUNDING

We thank the NOAA Office of Ocean Exploration (grant # NA17OAR0110209), the Gordon and Betty Moore Foundation

REFERENCES

- Becker, J. J., Sandwell, D. T., Smith, W. H. F., Braud, J., Binder, B., Depner, J., et al. (2009). Global bathymetry and elevation data at 30 Arc seconds resolution: SRTM30_PLUS. *Mar. Geod.* 32, 355–371. doi: 10.1080/01490410903297766
- Cappo, M., Harvey, E., and Shortis, M. (2006). "Counting and measuring fish with baited video techniques – an overview," *Proceedings of the Cutting-Edge Technologies in Fish and Fisheries Science*, 101–114. doi: 10.1007/978-1-62703-724-2_1
- Chao, A., Gotelli, N. J., Hsieh, T. C., Sander, E. L., Ma, K. H., Colwell, R. K., et al. (2014). Rarefaction and extrapolation with Hill numbers: a framework for sampling and estimation in species diversity studies. *Ecol. Monogr.* 84, 45–67. doi: 10.1890/13-0133.1
- Christiansen, B., Vieira, R. P., Christiansen, S., Denda, A., Oliveira, F., and Goncalves, J. M. S. (2015). The fish fauna of ampere seamount (NE Atlantic) and the adjacent abyssal plain. *Helgol. Mar. Res.* 69, 13–23. doi: 10.1007/s10152-014-0413-4
- Cuvelier, D., Ribeiro, P. A., Ramalho, S. P., Kersken, D., Martinez Arbizu, P., and Colaço, A. (2020). Are seamounts refuge areas for fauna from polymetallic nodule fields? *Biogeosciences* 17, 2657–2680. doi: 10.5194/bg-2019-304
- Denda, A., Stefanowitsch, B., and Christiansen, B. (2017). From the epipelagic zone to the abyss: trophic structure at two seamounts in the subtropical and tropical Eastern Atlantic - Part I zooplankton and micronekton. *Deep. Res. Part I Oceanogr. Res. Pap.* 130, 63–77. doi: 10.1016/j.dsr.2017.10.010
- Drazen, J. C., Leitner, A. B., Morningstar, S., Marcon, Y., Greinert, J., and Purser, A. (2019). Observations of deep-sea fishes and mobile scavengers from the abyssal DISCOL experimental mining area. *Biogeosciences* 16, 3133–3146. doi: 10.5194/bg-16-3133-2019
- Drazen, J. C., Smith, C. R., Gjerde, K. M., Haddock, S. H. D., Carter, G. S., Choy, C. A., et al. (2020). Midwater ecosystems must be considered when evaluating environmental risks of deep-sea mining. *Proc. Natl. Acad. Sci. U.S.A.* 117, 17455–17460. doi: 10.1073/pnas.2011914117
- Drazen, J. C., and Sutton, T. T. (2017). Dining in the deep: the feeding ecology of deep-sea fishes. *Ann. Rev. Mar. Sci.* 9, 1–26. doi: 10.1146/annurev-marine-010816-060543

(grant no. 5596), and the University of Hawaii School of Ocean and Earth Science and Technology (SOEST) for financial support. Open Access fees were funded by The Pew Charitable Trusts.

ACKNOWLEDGMENTS

We thank the captain and crew of the RV *Kilo Moana* and the science team of the DeepCCZ expedition for making this research possible. We thank taxonomic experts David G. Smith and Kenneth Tighe of the Smithsonian Institute for assistance with identification of all trapped specimens, and Ben Frable and Philip A. Hastings of the Scripps Institute of Oceanography fish collection for allowing us to examine the synphobranchid specimens archived there. We also thank Kirsty McQuaid and Kerry Howell for extracting the seafloor POC flux for our deployment locations from the Lutz et al. (2007) model. This is SOEST contribution #11380.

SUPPLEMENTARY MATERIAL

The Supplementary Material for this article can be found online at: <https://www.frontiersin.org/articles/10.3389/fmars.2021.636305/full#supplementary-material>

- Drazen, J. C., Leitner, A. B., Jones, D. O. B., and Simon-Lledó, E. (2021). Regional variation in communities of demersal fishes and scavengers across the Clarion Clipperton Zone and Pacific ocean. *Front. Mar. Sci.* (in press).
- Durden, J. M., Bett, B. J., Jones, D. O. B., Huvenne, V. A. I., and Ruhl, H. A. (2015). Abyssal hills – hidden source of increased habitat heterogeneity, benthic megafaunal biomass and diversity in the deep sea. *Prog. Oceanogr.* 137, 209–218. doi: 10.1016/j.pocean.2015.06.006
- Durden, J. M., Bett, B. J., and Ruhl, H. A. (2020). Subtle variation in abyssal terrain induces significant change in benthic megafaunal abundance, diversity, and community structure. *Prog. Oceanogr.* 186:102395. doi: 10.1016/j.pocean.2020.102395
- Durden, J. M., Ruhl, H. A., Pebody, C., Blackbird, S. J., and van Oevelen, D. (2017). Differences in the carbon flows in the benthic food webs of abyssal hill and plain habitats. *Limnol. Oceanogr.* 62, 1771–1782. doi: 10.1002/lno.10532
- Estes, J. A., Terborgh, J., Brashares, J. S., Power, M. E., Berger, J., Bond, W. J., et al. (2011). Trophic downgrading of planet Earth. *Science* 333, 301–306. doi: 10.1126/science.1205106
- Gehlenborg, N. (2019). *UpSetR: A More Scalable Alternative to Venn and Euler Diagrams for Visualizing Intersecting Sets*.
- Genin, A. (2004). Bio-physical coupling in the formation of zooplankton and fish aggregations over abrupt topographies. *J. Mar. Syst.* 50, 3–20.
- Genin, A., and Dower, J. F. J. (2007). "Seamount plankton dynamics," in *Seamounts: Ecology, Fisheries & Conservation*, eds T. J. Pitcher, T. Morato, P. J. B. Hart, M. R. Clark, N. Haggan, and R. S. Santos (Oxford: Blackwell Publishing), 85–100.
- Genin, A., Haury, L., and Greenblatt, P. (1988). Interactions of migrating zooplankton with shallow topography: predation by rockfishes and intensification of patchiness. *Deep Sea Res. Part A* 35, 151–175. doi: 10.1016/0198-0149(88)90034-9
- Gollner, S., Kaiser, S., Menzel, L., Jones, D. O. B., Brown, A., Mestre, N. C., et al. (2017). Resilience of benthic deep-sea fauna to mining activities. *Mar. Environ. Res.* 129, 76–101. doi: 10.1016/j.marenvres.2017.04.010
- Gove, J. M., McManus, M. A., Neuheimer, A. B., Polovina, J. J., Drazen, J. C., Smith, C. R., et al. (2016). Ocean Oases: near-island biological hotspots in barren ocean basins. *Nat. Commun.* 7, 1–34. doi: 10.1038/ncomms10581

- Hanski, I., Zurita, G. A., Bellocq, M. I., and Rybicki, J. (2013). Species-fragmented area relationship. *Proc. Natl. Acad. Sci. U.S.A.* 110, 12715–12720. doi: 10.1073/pnas.1311491110
- Harbour, R. P., Leitner, A. B., Ruehleemann, C., Vink, A., and Sweetman, A. K. (2020). Benthic and demersal scavenger biodiversity in the eastern end of the Clarion-clipperton Zone – An area marked for polymetallic nodule mining. *Front. Mar. Sci.* 7:458. doi: 10.3389/fmars.2020.00458
- Holland, K. N., and Grubbs, R. D. (2007). “Fish visitors to seamounts: tunas and billfish at seamounts,” in *Seamounts: Ecology, Fisheries and Conservation*, eds T. J. Pitcher, T. Morato, P. J. B. Hart, M. R. Clark, N. Haggan, and R. S. Santos (Oxford: Blackwell Publishing), 189–206.
- Hsieh, T. C., Ma, K. H., and Chao, A. (2016). iNEXT: an R package for rarefaction and extrapolation of species diversity (Hill numbers). *Methods Ecol. Evol.* 7, 1451–1456. doi: 10.1111/2041-210X.12613
- Jones, D. O. B., Kaiser, S., Sweetman, A. K., Smith, C. R., Menot, L., Vink, A., et al. (2017). Biological responses to disturbance from simulated deep-sea polymetallic nodule mining. *PLoS One* 12:e0171750. doi: 10.1371/journal.pone.0171750
- Kim, S.-S., and Wessel, P. (2011). New global seamount census from altimetry-derived gravity data. *Geophys. J. Int.* 186, 615–631. doi: 10.1111/j.1365-246X.2011.05076.x
- Laroche, O., Kersten, O., Smith, C. R., and Goetze, E. (2020). Environmental DNA surveys detect distinct metazoan communities across abyssal plains and seamounts in the western Clarion Clipperton Zone. *Mol. Ecol.* 29, 4588–4604. doi: 10.1111/mec.15484
- Lavelle, W. J., and Mohn, C. (2010). Motion, commotion, and biophysical connections at deep ocean seamounts. *Oceanography* 23, 90–103. doi: 10.5670/oceanog.2010.64
- Leitner, A. B., Durden, J. M., Smith, C. R., Klingberg, E. D., and Drazen, J. C. (2021). Synphobranchid eel swarms on abyssal seamounts: largest aggregation of fishes ever observed at abyssal depths. *Deep Sea Res. Part I Oceanogr. Res. Pap.* 167:103423. doi: 10.1016/j.dsr.2020.103423
- Leitner, A. B., Neuheimer, A. B., and Drazen, J. C. (2020). Evidence for long-term seamount-induced chlorophyll enhancements. *Sci. Rep.* 10, 1–10. doi: 10.1038/s41598-020-69564-0
- Leitner, A. B., Neuheimer, A. B., Donlon, E., Smith, C. R., and Drazen, J. C. (2017). Environmental and bathymetric influences on abyssal bait-attending communities of the Clarion Clipperton Zone. *Deep. Res. Part I Oceanogr. Res. Pap.* 125, 65–80. doi: 10.1016/j.dsr.2017.04.017
- Linley, T. D., Stewart, A. L., McMillan, P. J., Clark, M. R., Geringer, M. E., Drazen, J. C., et al. (2017). Bait attending fishes of the abyssal zone and hadal boundary: community structure, functional groups and species distribution in the Kermadec, New Hebrides and Mariana trenches. *Deep Sea Res. Part I Oceanogr. Res. Pap.* 121, 38–53. doi: 10.1016/j.dsr.2016.12.009
- Lundblad, E. R., Wright, D. J., Miller, J., Larkin, E. M., Rinehart, R., Naar, D. F., et al. (2006). A benthic terrain classification scheme for American Samoa. *Mar. Geod.* 29, 89–111. doi: 10.1080/01490410600738021
- Lutz, M. J., Caldeira, K., Dunbar, R. B., and Behrenfeld, M. J. (2007). Seasonal rhythms of net primary production and particulate organic carbon flux to depth describe the efficiency of biological pump in the global ocean. *J. Geophys. Res.* 112:C10011. doi: 10.1029/2006JC003706
- Mcquaid, K. A., Attrill, M. J., Clark, M. R., Copley, A., Glover, A. G., Smith, C. R., et al. (2020). Using habitat classification to assess representativity of a protected area network in a large, data-poor area targeted for deep-sea mining. *Front. Mar. Sci.* 7, 1–21. doi: 10.3389/fmars.2020.558860
- Milligan, R. J., Morris, K. J., Bett, B. J., Durden, J. M., Jones, D. O. B., Robert, K., et al. (2016). High resolution study of the spatial distributions of abyssal fishes by autonomous underwater vehicle. *Sci. Rep.* 6, 1–12. doi: 10.1038/srep26095
- Modeler, B. T. (2012). Benthic terrain modeler v3.0 for ArcGIS 10.x. *ESRI* 2012, 1–14.
- Morato, T., Bulman, C., and Pitcher, T. J. (2009). Modelled effects of primary and secondary production enhancement by seamounts on local fish stocks. *Deep Sea Res. Pt. II* 56, 2713–2719.
- Morato, T., Hoyle, S. D., Allain, V., and Nicol, S. J. (2010). Seamounts are hotspots of pelagic biodiversity in the open ocean. *Proc. Natl. Acad. Sci. U.S.A.* 107, 9707–9711. doi: 10.1073/pnas.0910290107
- Morris, K. J., Bett, B. J., Durden, J. M., Benoist, N. M. A., Huvenne, V. A. I., Jones, D. O. B., et al. (2016). Landscape-scale spatial heterogeneity in phytodetrital cover and megafauna biomass in the abyss links to modest topographic variation. *Sci. Rep.* 6:34080. doi: 10.1038/srep34080
- Mullineaux, L. S., and Mills, S. W. (1997). A test of the larval retention hypothesis in seamount-generated flows. *Deep. Res. Part I Oceanogr. Res. Pap.* 44, 745–770. doi: 10.1016/S0967-0637(96)00130-6
- Myers, R. A., Baum, J. K., Shepherd, T. D., Powers, S. P., and Peterson, C. H. (2007). Cascading Effects of the Loss of Apex Predatory Sharks from a Coastal Ocean. *Science* 315, 1846–1850. doi: 10.1126/science.1138657
- National Oceanic & Atmospheric Administration (NOAA), and National Aeronautics and Space Administration (NASA) (n.d.). *Chlorophyll-a, Aqua MODIS, NPP, 4km, Science Quality, 2003-present (Monthly Composite)*.
- Oksanen, J., Blanchet, F. G., Kindt, R., Legendre, P., Minchin, P. R., O'Hara, R. B., et al. (2015). *vegan: Community Ecology Package*.
- Pitcher, T. J., Morato, T., Hart, P. J. B., Clark, M. R., Haggan, N., and Santos, R. S. (Eds). (2007). *Seamounts: Ecology, Fisheries and Conservation*. Blackwell Fisheries and Aquatic Resources Vol. 12 (Oxford: Blackwell Publishing).
- Polovina, J. J., Abecassis, M., Howell, E. A., and Woodworth, P. (2009). Increases in the relative abundance of mid-trophic level fishes concurrent with declines in apex predators in the subtropical North Pacific, 1996-2006. *Fish. Bull.* 107, 523–531.
- Priede, I. (2017). *Deep-Sea Fishes: Biology, Diversity, Ecology and Fisheries*. Cambridge: Cambridge University Press.
- Riehl, T., Wölfl, A.-C., Augustin, N., Devevy, C. W., and Brandt, A. (2020). Discovery of widely available abyssal rock patches reveals overlooked habitat type and prompts rethinking deep-sea biodiversity. *Proc. Natl. Acad. Sci.* 117, 15450–15459. doi: 10.1073/pnas.1920706117
- Rowden, A. A., Dower, J. F., Schlacher, T. A., Consalvey, M., and Clark, M. R. (2010). Paradigms in seamount ecology: fact, fiction and future. *Mar. Ecol.* 31, 226–241. doi: 10.1111/j.1439-0485.2010.00400.x
- Rybicki, J., and Hanski, I. (2013). Species-area relationships and extinctions caused by habitat loss and fragmentation. *Ecol. Lett.* 16, 27–38. doi: 10.1111/ele.12065
- Schlacher, T. A., Rowden, A. A., Dower, J. F., and Consalvey, M. (2010). Seamount science scales undersea mountains: new research and outlook. *Mar. Ecol.* 31, 1–13. doi: 10.1111/j.1439-0485.2010.00396.x
- Simon-Lledó, E., Bett, B. J., Huvenne, V. A. I., Köser, K., Schoening, T., Greinert, J., et al. (2019). Biological effects 26 years after simulated deep-sea mining. *Sci. Rep.* 9, 1–13. doi: 10.1038/s41598-019-44492-w
- Smith, C. R., De Leo, F. C., Bernardino, A. F., Sweetman, A. K., and Arbizu, P. M. (2008). Abyssal food limitation, ecosystem structure and climate change. *Trends Ecol. Evol.* 23, 518–528.
- Smith, C. R., Tunnicliffe, V., Colaço, A., Drazen, J. C., Gollner, S., Levin, L. A., et al. (2020). Deep-sea misconceptions cause underestimation of seabed-mining impacts. *Trends Ecol. Evol.* 35, 853–857. doi: 10.1016/j.tree.2020.07.002
- Verfaillie, E., Doornenbal, P., Mitchel, A. J., White, J., and Van Lancker, V. (2007). *The Bathymetric Position Index (BPI) as a Support Tool for Habitat Mapping, Mapping European Seabed Habitats*. Available online at: [http://www.emodnet-seabedhabitats.eu/PDF/GMHM4_Bathymetric_position_index_\(BPI\).pdf](http://www.emodnet-seabedhabitats.eu/PDF/GMHM4_Bathymetric_position_index_(BPI).pdf) (accessed February 06, 2017).
- Vieira, R. P., Coelho, R., Denda, A., Martin, B., Gonçalves, J. M. S., and Christiansen, B. (2018). Deep-sea fishes from Senghor Seamount and the adjacent abyssal plain (Eastern Central Atlantic). *Mar. Biodivers.* 48, 963–975. doi: 10.1007/s12526-016-0548-4
- Washburn, T. W., Jones, D. O. B., Wei, C. L., and Smith, C. R. (2021). Environmental heterogeneity throughout the clarion-clipperton zone and the potential representativity of the APEI network. *Front. Mar. Sci.* 8:661685. doi: 10.3389/fmars.2021.661685
- Wedding, L. M., Friedlander, A. M., Kittinger, J. N., Watling, L., Gaines, S. D., Bennett, M., et al. (2013). From principles to practice: a spatial approach to systematic conservation planning in the deep sea. *Proc. Biol. Sci.* 280:20131684. doi: 10.1098/rspb.2013.1684
- Wedding, L. M., Reiter, S. M., Smith, C. R., Gjerde, K. M., Kittinger, J. N., Friedlander, A. M., et al. (2015). Managing mining of the deep seabed. *Science* 349, 144–145. doi: 10.1126/science.aac6647

- Wessel, P. (2001). Global distribution of seamounts inferred from gridded Geosat/ERS-1 altimetry. *J. Geophys. Res.* 106:19431.
- Wessel, P., Sandwell, D. T., and Kim, S.-S. (2010). The global seamount census. *Oceanography* 23, 24–33.
- Whitaker, D., and Christman, M. (2014). *clustsig: Significant Cluster Analysis*.
- Wilson, R. R. Jr., Smith, K. L. Jr., and Rosenblatt, R. H. (1985). Megafauna associated with bathyal seamounts in the central North Pacific Ocean. *Deep Sea Res. Part A. Oceanogr. Res. Pap.* 32, 1243–1254. doi: 10.1016/0198-0149(85)90007-X
- Witte, U. (1999). Consumption of large carcasses by scavenger assemblages in the deep Arabian Sea: observations by baited camera. *Mar. Ecol. Prog. Ser.* 183, 139–147. doi: 10.3354/meps183139
- Yesson, C., Clark, M. R., Taylor, M. L., and Rogers, A. D. (2011). Deep-sea research I the global distribution of seamounts based on 30 arc seconds bathymetry data. *Deep. Res. Part I* 58, 442–453. doi: 10.1016/j.dsr.2011.02.004
- Ziegler, A. F., Cape, M., Lundesgaard, Ø, and Smith, C. R. (2020). Intense deposition and rapid processing of seafloor phytodetritus in a glaciomarine fjord, Andvord Bay (Antarctica). *Prog. Oceanogr* 187:102413. doi: 10.1016/j.pocean.2020.102413
- Conflict of Interest:** The authors declare that the research was conducted in the absence of any commercial or financial relationships that could be construed as a potential conflict of interest.
- Publisher's Note:** All claims expressed in this article are solely those of the authors and do not necessarily represent those of their affiliated organizations, or those of the publisher, the editors and the reviewers. Any product that may be evaluated in this article, or claim that may be made by its manufacturer, is not guaranteed or endorsed by the publisher.

Copyright © 2021 Leitner, Drazen and Smith. This is an open-access article distributed under the terms of the Creative Commons Attribution License (CC BY). The use, distribution or reproduction in other forums is permitted, provided the original author(s) and the copyright owner(s) are credited and that the original publication in this journal is cited, in accordance with accepted academic practice. No use, distribution or reproduction is permitted which does not comply with these terms.